



**The Massachusetts Toxics Use
Reduction Institute
University of Massachusetts
Lowell**

Green(er) PVC: The Development of Lead- and Phthalate-Free Nanocomposite Formulations with Practical Utility

**Toxics Use Reduction Institute
University Research in Sustainable Technologies Program**

Technical Report No. 60

2007

University of Massachusetts Lowell

Green(er) PVC: The Development of Lead- and Phthalate-Free Nanocomposite Formulations with Practical Utility

**Gowri Dorairaju, Mukthiar Basha Bukhari,
Gregory Morose and Asst. Prof. Daniel Schmidt**
Department of Plastics Engineering
University of Massachusetts Lowell

Project Manager: Pam Eliason
Toxics Use Reduction Institute

The Toxics Use Reduction Institute
University Research in Sustainable Technologies Program

2007

The Massachusetts Toxics Use Reduction Institute
University of Massachusetts Lowell



All rights to this report belong to the Toxics Use Reduction Institute. The material may be duplicated with permission by contacting the Institute.

The Toxics Use Reduction Institute is a multi-disciplinary research, education, and policy center established by the Massachusetts Toxics Use Reduction Act of 1989. The Institute sponsors and conducts research, organizes education and training programs, and provides technical support to promote the reduction in the use of toxic chemicals or the generation of toxic chemical byproducts in industry and commerce. Further information can be obtained by writing to the Toxics Use Reduction Institute, University of Massachusetts Lowell, One University Avenue, Lowell, Massachusetts 01854.

University Research in Sustainable Technologies

The University Research in Sustainable Technologies program is a project of the Toxics Use Reduction Institute (TURI). The program taps the research capabilities of the University of Massachusetts to advance the investigation, development and evaluation of sustainable technologies that are environmentally, occupationally and economically sound. Annually the program provides research funding to UMass faculty from all campuses on a competitive basis, and encourages faculty/industry partnerships and cross-campus collaboration. Industry partners provide guidance, propose applications for new technologies and, in some cases, evaluate and/or adopt processes and technologies resulting from research.

Past projects supported by this program have focused on finding alternatives to the use of toxic chemicals in the wire and cable industry. These projects, which are described in more detail on TURI's website (go to www.turi.org and click on Industry, Research, University Research in Sustainable Technologies, Wire and Cable Projects), include:

- 2006 – Improved Lead-Free Wire and Cable Insulation Performance Using Nanocomposites – Asst. Prof. Daniel Schmidt and Noble Francis, UMass Lowell Department of Plastics Engineering.
- 2005 – Flame Retardancy Enhancement for EPDM Wire and Cable Coatings Using Nanoclays – Prof. Joey Mead, UMass Lowell Department of Plastics Engineering.
- 2004 – Alternative Stabilizers and Surface Characterization (SEM/EDXS Analysis) of EPDM for Wire and Cable Applications – Prof. Joey Mead, UMass Lowell Department of Plastics Engineering, and Changmo Sung, UMass Lowell Department of Chemical Engineering.
- 2003 – Analysis of Lead-Containing Wire Coating Materials – Prof. Joey Mead, UMass Lowell Department of Plastics Engineering, and Changmo Sung, UMass Lowell Department of Chemical Engineering.
- 2003 – Innovative Materials for Wire and Cable Coating – Prof. Stephen McCarthy, UMass Lowell Department of Plastics Engineering and the Institute for Plastics Innovations.
- 2002 – Innovative Materials for Wire and Cable Coating – Prof. Stephen McCarthy, UMass Lowell, Department of Plastics Engineering and the Institute for Plastics Innovations.

Executive Summary

All materials have the potential to cause both positive and negative impacts on human health and the environment, and poly vinyl chloride (PVC) is certainly no exception. Filling the needs of end users while minimizing the hazards associated with PVC based materials is becoming increasingly challenging for the plastics industry. The use of lead stabilizers and phthalate plasticizers in PVC wire and cable formulations in particular is a significant problem in this regard.

The goal of this project is the production of high-performance, lead- and phthalate-free PVC compounds for wire and cable insulation, which addresses the serious environmental issues surrounding the use of their leaded counterparts, providing a lower-toxicity alternative to current materials. Clay nanocomposite technology has been selected as a means to achieve this goal, as it has been demonstrated that such systems can improve a variety of properties relevant to the performance of wire and cable insulation (thermal stability, barrier properties, flame retardance, etc.). The researchers chose environmentally benign clay nanofillers and vegetable oil-based plasticizers, and looked for synergistic interactions between the two additives that are expected due to the excellent dispersability of nanoclays in epoxidized vegetable oil and the stabilizing effects reported for both additives.

Based on materials and a realistic wire and cable formulation provided by the research industrial partner, Teknor Apex, PVC was dry-blended with various stabilizers (lead and non-lead) and plasticizers (diisodecyl phthalate, DIDP, and epoxidized linseed oil, ELO), compounded using a twin-screw extruder with and without a low loading of nanoclay (chosen based on past work with FPVC nanocomposites), pelletized, and sheet extruded for properties analysis. The results of these analyses indicate that ELO is at least as effective as DIDP with the non-lead stabilizers, giving similar or improved mechanical and electrical properties at identical loading levels. In addition to mechanical and electrical properties, thermal and fire testing results are also reported for these materials and their nanocomposites.

Table of Contents

University Research in Sustainable Technologies.....	i
Executive Summary.....	ii
1. Project Background / Description.....	1
2. Research Objectives.....	6
3. Experimental.....	7
3.1 Materials.....	7
3.2. Processing.....	9
3.2.1. Preparation of PVC / OMMT nanocomposites – Conventional dry-blending .	9
3.2.2. Melt Blending of FPVC / OMMT nanocomposites – Twin screw extrusion.	10
3.2.3. Sheet Extrusion of PVC / OMMT nanocomposites.....	11
3.2.4. Compression Molding of PVC / OMMT nanocomposites.....	12
3.3. Monitoring of Nanoparticles.....	12
3.4. Testing.....	14
3.4.1. Thermal Stability.....	14
3.4.2. Mechanical Properties.....	15
3.4.3. Electrical Properties.....	16
3.4.4. Fire Properties.....	16
3.4.5. Plasticizer Extraction Test.....	17
4. Results and Discussions.....	18
4.1. Processing.....	18
4.1.1. Dry Blending.....	18
4.1.2. Melt compounding.....	18
4.1.3. Sheet extrusion.....	18
4.2. Nanoparticle monitoring.....	19
4.3. Testing.....	24
4.3.1. Thermal Stability.....	24
4.3.2. Mechanical Properties.....	29
4.3.3. Electrical Properties.....	35
4.3.4. Fire Properties.....	38
4.3.5. Plasticizer Extraction Test.....	40
5. Conclusions.....	40
Acknowledgements.....	44
References.....	45
Appendices.....	58

1. Project Background/Description

Poly (vinyl chloride) (PVC) is not normally thought of as an environmentally friendly plastic. Commercial PVC formulations must be thermally stabilized and plasticized before they can be used in most applications. This lack of thermal stability combined with the great range of additives that may be present in a particular formulation makes recycling of PVC products difficult. Historically speaking, lead compounds and phthalates have been the cheapest, most effective classes of thermal stabilizers and plasticizers used in PVC products. Therefore, despite the known and suspected negative effects on health and the environment associated with these additives, and the significant potential for exposure to these compounds that such formulations represent, these compounds continue to be used in a variety of PVC-based products. According to 1999 TURA data¹, the insulation industry in Massachusetts alone used nearly 3.5 million pounds of lead compounds. This represents a serious environmental concern for industry in Massachusetts, and is indicative of the concern for industry throughout the country as a whole. As the health and environmental hazards of PVC additives have been more fully characterized, significant efforts have been made to find replacements for both families of compounds.

Lead-free thermal stabilizers (barium and cadmium based stabilizers for instance) can themselves be quite toxic, and in spite of their increased cost do not deliver the same levels of performance of the lead salts they replace. For wire and cable insulation applications, the use of alternatives to lead stabilizers has been slow to be adopted because these other compounds do not consistently meet the most stringent flame retardancy standards. Nevertheless, and largely in response to demand from European customers who cannot use lead in their products in accordance with the EU Restriction on the Hazardous Substance (RoHS) Directive, some lead-free, low toxicity alternatives are currently on the market. Teknor Apex, a Massachusetts-based compounder of PVC resins, announced in May 2005 that it has “the broadest range of non-lead stabilized (NLS) vinyl compounds available to the wire and cable industry, enabling companies to manufacture products that comply with the European Union’s upcoming ‘RoHS’ legislation.”

With respect to plasticizers, phthalates represent the most efficient plasticizers for PVC, and the price to performance ratio of phthalates is particularly favorable for low profit margin industries such as the wire and cable industry. Alternative plasticizers are available, but one-to-one substitutions for phthalates tend to add expense and often result in an unacceptable reduction in performance. Still, the fact remains that PVC is an inexpensive and versatile plastic; as such, it is highly unlikely that it will be completely replaced in the near future. With that in mind, the goal of the work is to produce high-performance lead- and phthalate-free flexible PVC (FPVC) compounds for wire and cable insulation.

Lead- and phthalate-free compositions are further enhanced with respect to their performance and practical utility through the addition of a small amount of organically modified clay, to form a layered silicate nanocomposite – an approach that has future utility in non-PVC based formulations as well. The idea is to take advantage of an effect already demonstrated commercially by Honeywell’s Aegis nanocomposite barrier Nylon-6 resins². The barrier component of these resins is polyamide containing both organically modified clay and an oxygen scavenger. Dispersed clay platelets alone improve barrier properties thanks to their high aspect ratio and impermeability, which forces diffusing species to take a highly tortuous path in order to pass through the material. Oxygen scavengers, on the other hand, chemically consume oxygen as it attempts to diffuse through the material. While neither one gives an oxygen permeability low enough to compete with glass, when combined, they do exactly that, thanks to a synergistic effect. Simply put, the longer diffusion path that the clay forces the oxygen to take greatly improves the chances that oxygen and the oxygen scavengers will meet, giving the oxygen scavengers more time to do their work.

In the case of wire and cable insulation, PVC-based compositions thermally degrade by “zip dechlorohydration³”, as shown in Figure 1.

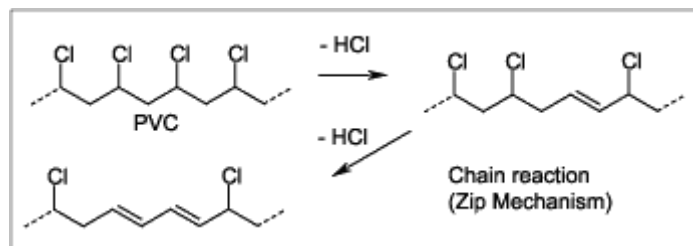


Figure 1 – Zip dechlorohydration as it occurs during the thermal degradation of poly(vinyl chloride); such degradation becomes visually evident through discoloration of the polymer when uninterrupted sequences of at least 4-6 consecutive double bonds form^{4,5,6}.

Structural defects in the PVC and the presence of oxygen, acids or bases (including HCl itself) both accelerate this degradation. This effect is readily apparent; discoloration of the polymer occurs as numerous double bonds are formed and highly conjugated molecules appear. Such highly conjugated molecules, in turn, tend not only to have increased electrical conductivity compared to the original polymer, but are also very sensitive to oxidative degradation. The end result is a dramatic degradation in the physical, mechanical, and electrical properties of the insulation material. Stabilizers slow this process by coupling with defects or double bonds formed as a result of dechlorohydration, by scavenging acids or bases from the system, or by acting as antioxidants. The addition of clays to such a system allows for a number of specific enhancements with respect to what such stabilizers already accomplish. From the aforementioned case of the Nylon-6 oxygen barrier films, it is clear that dispersed clays can increase scavenging efficiency; the same effects with respect to HCl scavenging can therefore be expected here. Finally, in addition to the enhanced thermal stability often seen in polymer/clay nanocomposites in general, an additional advantage often seen in these systems is their inherent flame retardance due to formation of silicate char once burning begins at an exposed surface.

These factors give the producer some attractive choices. Thermal stability and flame retardance may be improved, and the overall performance of the formulation therefore enhanced, with the addition of the primary stabilizer. Alternatively, if the performance is already acceptable without the clays, their addition may allow for a reduction in the concentration of primary stabilizer, which could result in reduced costs and/or issues of toxicity, depending on the compound in use. Finally, amounts of flame-

retardants might also be reduced in nanocomposite formulations. It is not enough simply to produce such materials; they must be accepted and used as widely as possible to facilitate the elimination of leaded formulations.

The next step is to address the issue of phthalate plasticizers in these same formulations. As noted previously, phthalates are both cheap and effective. Di (2-ethylhexyl) phthalate (DEHP), sometimes referred to as di (octyl) phthalate (DOP), has received the most scrutiny. While there is some controversy over exactly how toxic this and other phthalates are, these compounds as a class have been identified as endocrine disruptors⁷, and DEHP in particular has been indicated as a suspected carcinogen capable of causing harm to the reproductive organs, lungs, kidney and liver, and has been shown to cross the placenta to embryos and to appear in breast milk⁸. Because of concern over the potential effects of near-lifelong exposures to low levels of such compounds, the European Union has taken steps to substantially reduce the use of phthalates in certain applications, including children's toys. In addition, phthalates are petroleum derivatives, which give rise to questions of their long-term sustainability. Their cost remains fairly low for the moment, but demand for petroleum will only increase even as recent events expose the issue of supply as more critical than ever before.

In addition to handling hazards, DEHP is too volatile for wire and cable compounds⁹. The work has therefore involved diisodecyl phthalate (DIDP), a similar but less mobile member of the phthalate family. It, like many other plasticizers, has limited thermal stability in its own right, and must be protected by antioxidants in order to remain heat stable. This system is therefore a perfect test-bed to examine the effects of plasticizer replacement on the properties of a high-performance PVC formulation.

The best candidates identified for use as phthalate replacements, from the standpoint of performance and sustainability, are epoxidized vegetable oils¹⁰. Epoxidized linseed oil (ELO) in particular has been identified as an appropriate substitute, based on a number of advantages this compound possesses. From the standpoint of performance, PVC formulations containing epoxidized vegetable oils exhibit greater stability with respect to heat^{11,12,13,14,15,16,17,18}, light¹¹, and gamma irradiation^{19,20,21,22,23,24,25,26}, potentially obviating the need for additional antioxidant additives and offering further protection to the polymer. Epoxy groups are effective HCl scavengers^{15,19,21,27}, meaning that such epoxidized oils will act not only as highly stable plasticizers but will hinder the

HCl-catalyzed degradation of PVC as it undergoes thermally induced dechlorohydration according to the mechanism shown in Figure 1²⁸.

Epoxidized vegetable oils also have higher molecular weights than the usual petroleum-derived plasticizers (e.g., phthalates, sebacates, adipates and trimellitates), making them much harder to extract and much less likely to volatilize, and ensuring they remain in the PVC as so-called “permanent” plasticizers²⁹. In addition to the obvious advantages of minimal extractability from the standpoint of both the retention of properties and the prevention of migration to the surroundings, the reduced mobility due to increased molecular weight also gives these compounds in general (and ELO in particular) an advantage when low conductivity is desired (as in electrical applications)³⁰ and may reduce the flammability of these compounds, given that plastics generally burn via the volatilization of combustible additives and/or degradation products.

For all of these reasons epoxidized soybean oil (ESO) is already used in a variety of vinyl formulations, including high-performance wire and cable compounds^{31,32,33,34,35}. ESO is not sufficiently miscible with PVC to be considered a primary plasticizer, however; this, in fact, is the Achilles heel of many such epoxidized vegetable oils^{10,36,37}. ELO is the exception³⁷; this compound represents the only commercial epoxidized vegetable oil that can be used as a primary plasticizer in PVC formulations. From a more practical point of view, availability of ELO is excellent, with a number of companies already in commercial production^{38,39,40,41,42,43,44}. Finally, while the cost of epoxidized vegetable oils is higher than their phthalate counterparts, because they have the potential to reduce the need for potentially costly antioxidants and thermal stabilizers, and because they may be more efficient in plasticizing PVC than a number of other compounds⁴⁵ and may also give improved low-temperature flexibility, the possibility exists to produce effectively ELO-plasticized formulations with an excellent price to performance ratio, making their acceptance more practical¹⁰.

The next question is whether or not ELO will be compatible with nanoclays of the type we have previously studied and successfully used in the production of PVC nanocomposites. In fact, the specific organoclay chosen for our work, Southern Clay’s Cloisite 30B, is known to show excellent compatibility with epoxy resins thanks to the presence of hydroxyethyl groups in the alkylammonium modifier used to compatibilize

the clay nanolayers with the polymer matrix (shown below, Figure 2); these hydroxyethyl groups interact with epoxies on a molecular level to enhance silicate dispersion^{46,47,48}.

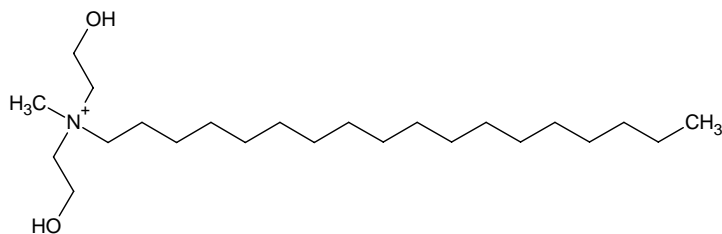


Figure 2 – The structure of the bis (2-hydroxyethyl) methyl tallow ammonium modifier present in Cloisite 30B, organically modified Montmorillonite clay produced by Southern Clay Products for nanocomposite formation and previously studied in combination with plasticized lead-free PVC formulations.

Epoxy compounds have already shown promise as additives to improve dispersion levels in PVC nanocomposites^{49,50}, while recent studies show that mixtures of Cloisite 30B and ELO-based epoxies give rise to high levels of dispersion, down to the level of individual clay nanolayers^{51,52,53}. These results show that ELO is not just compatible with the nanoclay, but is optimally suited for combination with it, and may in fact improve the level of clay dispersion even further.

As noted previously, it is not enough to produce a more environmentally acceptable solution if it is not also accepted by the market. Based on the arguments herein, the goal of our work is to develop lead-free, phthalate-free formulations that display mechanical, thermal, and barrier performance characteristics appropriate for application as wire and cable compounds without drastically affecting the cost. PVC will never be truly “green”, but success in this work will provide the basis for far greener formulations than currently exist, and will help us make the most of an extremely versatile commodity plastic while minimizing harm to the populace and the environment.

2. Research Objectives

Polymer nanocomposites represent a new and promising area of polymer research. Among the particles used to form nanocomposites, organically modified clays are of particular interest. In such systems, the combination of high aspect ratio clay mono- or multi-layers and their interactions with the matrix polymer can lead to improvements in barrier, thermal, and mechanical properties at far lower loading levels

than are typically used in conventional filled polymer composites^{54, 55, 56}. In this work we seek to produce lead- and phthalate-free melt-blended PVC nanocomposites with performance appropriate for wire and cable formulations. We intend to investigate improvements in properties related to physical, environmental, and thermal stability and flame retardance, while retaining if not improving the volume resistivity, mechanical flexibility and toughness required for wire and cable applications. In addition, air monitoring was conducted to evaluate the potential for occupational exposure to nanoparticles during processing.

The overall objective of this work will be to develop lead- and phthalate-free PVC formulations without substantial penalties with respect to price-to-performance ratio in order to address the issue of market acceptance as well as materials characteristics. In the absence of strong government oversight, the production of lead- and phthalate-free alternatives is only part of the solution; only when such alternative formulations are widely used will the issue of lead and phthalate in wire and cable insulation be properly addressed.

3. Experimental

3.1 Materials

A suspension grade of Georgia Gulf PVC resin 2100 (K ~ 67) was procured from Teknor Apex and was used as received (denoted as *R* in Appendix A) in the form of a colorless free-flowing powder.

Five different kinds of stabilizers were chosen for the study – one standard lead-based stabilizer and four non-lead based stabilizers were. All stabilizers were provided by Teknor Apex. Halstab 60 was used as the lead-based stabilizer (Pb), and consists of a blend of tribasic lead sulfate and dibasic lead phthalate. This stabilizer was used as the control stabilizer in this study. Non-Pb 1 consists of a mixture of Ca, Mg, and Zn based solids. Non-Pb 2 contains Ca and Zn only. The other two non-lead based stabilizers used in the study, non-Pb 3 and non-Pb 4, also act as lubricants. The former is a solid mixed-metal system. The latter is a Ca / Zn based solid stabilizer. All stabilizers were used as-received, in the form of colorless, powders.

Two different plasticizers were used in this study: Diisodecyl phthalate (DIDP) and Vikoflex 7190 epoxidized linseed oil (ELO, purchased from Arkema). DIDP was provided by Teknor Apex, and both were used as received (in the form of clear, colorless, viscous liquids). Figure 3 illustrates the chemical structures of DIDP and ELO.

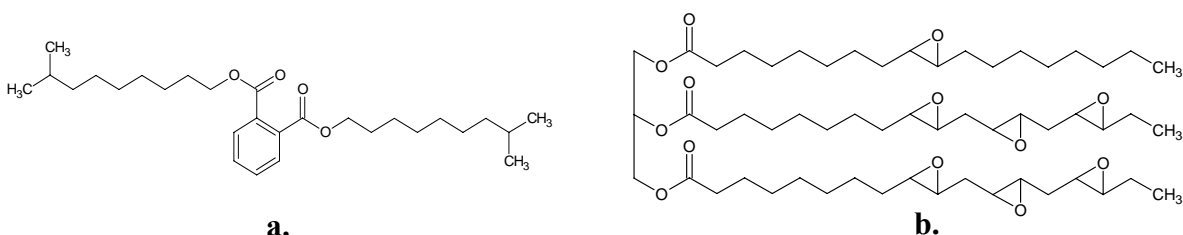


Figure 3 – The chemical structures of **a.** diisodecyl phthalate (DIDP), and **b.** Epoxidized linseed oil (ELO)⁴⁵.

The organophilic montmorillonite (OMMT) clay used in this research, Southern Clay's Cloisite 30B (denoted as *OMMT* in Appendix A) was used as received (in the form of a beige, free-flowing powder). *OMMT* was chosen for evaluation based on numerous literature reports indicating excellent compatibility with PVC and improved thermal and mechanical properties in melt-blended systems^{57,58,59,60,61,62,63,64}. These reports were previously confirmed by this research group, with materials produced demonstrating substantial chemical compatibility between polymer and clay as well as significant improvements in oxygen barrier at very low clay concentrations without compromising mechanical properties or processability. *OMMT* consists of montmorillonite layers modified by the methyl tallow bis (2-hydroxyethyl) ammonium cation (MT2EtOH). The chemical structure of this modifier is shown in Figure 2. Note that in the free form the clay modifiers are present as chloride salts, while in the ion-exchanged form negative charges from the clay layers acts as counter-ions instead.

Fillers chosen for the study were Essen's antimony trioxide (added as a fire retardant), Imerys ATOMITE (calcium carbonate) and Engelhard Satintone SP-33 (kaolin). All materials were supplied by Teknor Apex, and used as received in the form of powders. These fillers were chosen to mimic the formulations used for wire and cable applications, based on information provided by Teknor Apex.

Crompton's Industrene R, which served as the lubricant, was provided by Teknor Apex and used as received in the form of colorless flakes.

3.2. Processing

3.2.1. Preparation of PVC / OMMT nanocomposites – Conventional dry-blending

Commercial PVC compounds were dry blended in a conventional high speed mixer. All fillers were dried at a temperature of 80 °C for 2 hours to completely remove moisture. The individual materials were weighed according to the original formulation (refer to Appendix B). The PVC resin and the stabilizer were added into the mixer at an initial temperature of 65°F (18 °C). The blade speed was set at 18 rpm and then slowly increased to 22 rpm and then to 30 rpm. At 180°F (82°C), the blade speed was decreased to 18 rpm and then the plasticizer was added into the blend. Similarly, the fillers (clay, flame retardants, extenders) and lubricants were added at 190°F (88°C) and 205°F (96°C), respectively. When a temperature of 215°F (102°C) was reached, water was supplied to the cooling jacket of the mixer. Once the temperature was reduced to 70°F (21°C), the blend was discharged from the mixer. By this technique 18 different compounds (Samples *A* to *R*, Appendix A) were dry-blended. Figure 4 (below) shows the equipment used in the dry blending process.



Figure 4 – Equipment used for dry-blending (Henschel high-intensity mixer).

3.2.2. Melt Blending of FPVC / OMMT nanocomposites – Twin screw extrusion

The dry-blended compounds were mixed homogeneously and extruded using a twin screw extruder (Mfg: Werner & Pfliederer / W&P, model ZSK-30, L/D: 32:1, diameter: 30 mm). Low shear PVC screw programming (refer to Appendix C) was used for all compounds. The temperature profile of the extruder from the hopper to the die was maintained at 140°C, 140°C, 150°C, 155°C and 165°C. The powders were fed into the hopper using a small volumetric feeder. The powders were conveyed through the various zones of the screw and were sheared and melted inside the barrel. The melt emerging from the single strand die was cooled underwater and then granulated into small cylindrical pellets using a pelletizer (Mfg: Conair). The optimized processing conditions for each compound (Samples *A* to *R*) are shown in Appendix D. Figure 5 shows the equipment used for melt compounding.



Figure 5 – Equipment used for melt compounding (Werner & Pfliederer ZSK-30 twin-screw extruder).

3.2.3. Sheet Extrusion of PVC / OMMT nanocomposites

The extruded PVC / OMMT granules were sheet-extruded using a single-screw sheet extruder (Mfg: Welex). A coat hanger sheet die was used for extrusion. The pellets were gravimetrically fed into the hopper and were then conveyed to the feed, compression, and metering zones of the screw, respectively. The melt emerging from the sheet die was passed between chill rolls for cooling, which were maintained at a temperature of 80-100°C. Nip rolls were used for stretching, and the samples were collected as rolls using a winder. The temperature profile of the extruder from the feed throat to the die was maintained at 270°F (132°C), 300 °F (149°C), 335°F (168°C), 340°F (171°C), 340°F (171°C), and 340°F (171°C). The optimized processing conditions and thicknesses of each compound (Samples *A* to *R*) are given in Appendix D. Figure 6 shows the equipment used for sheet extrusion.



Figure 6 – Equipment used for sheet extrusion (Welex single-screw sheet extruder).

3.2.4. Compression Molding of PVC / OMMT nanocomposites

Extruded sheets of the each compound were compressed together via compression molding using a manual hydraulic press (Mfg: Carver, Model No: 3912) to obtain sheets with thicknesses of 3 mm. The top and bottom platen temperatures were maintained at 350°F (177°C). A 3 mm mold was used. The plates were cleaned and the sheets were placed between them, and then compressed with a low force (100 pounds) for 3 minutes, so as to transfer the heat to the sheet, before forces of 6,300 pounds and 10,000 pounds were applied for 3 min and 2 minutes respectively, to fuse the plies together and form the final sample. The plates were then removed from the platens and the samples were cooled at room temperature. Figure 7 shows the equipment used for compression molding.



Figure 7 – Equipment used for compression molding (Carver press).

3.3. Monitoring of Nanoparticles

The basis for the nanoclay described here is the naturally occurring mineral montmorillonite. The individual plate thickness is 1 nanometer and the lateral dimensions are generally 75 to 100 nanometers⁶⁵, resulting in a very high aspect ratio. Cloisite 30B, is a natural montmorillonite modified that has been purified and subsequently modified

with a quaternary alkylammonium salt. The typical dry particle size distribution of this material (by volume) is reported as follows⁶⁶:

- 10% are less than 2 microns
- 50% are less than 6 microns
- 90% are less than 13 microns

In order to assess the potential for worker exposure during processing, airborne nanoparticle concentrations were measured using a TSI Fast Mobility Particle Sizer Spectrometer (FMPS) during nanocomposite production, including real-time measurements during materials handling, dry blending, and melt extrusion. A P100 mask and neoprene gloves were worn as protection during these experiments.

The FMPS uses 32 channels to measure aerosol particles in the range from 5.6 to 560 nanometers in diameter. The instrument continuously draws air into the inlet, where particles are positively charged to a predictable level using a corona charger. The charged particles are then introduced to the measurement region along a vertically oriented high voltage electrode. A positive voltage is applied to the electrode creating an electric field that repels the charged particles towards electrometers. A charged particle with high electrical mobility strikes the electrometer near the top, and a charged particle with low electrical mobility strikes the electrometer near the bottom. Figure 8 shows the FMPS equipment collecting background data.



Figure 8 – FMPS equipment collecting background data

Appendix E shows the time, activity, and measurement location recorded during materials handling, dry blending and melt extrusion.

3.4. Testing

3.4.1. Thermal Stability

a) Thermogravimetric Analysis (TGA)

Specimen specification:

Shape: Pellets

Thermal decomposition studies were performed using a TGA (TA Instruments Q50). Samples (generally ~15-40 mg in mass) were placed in a platinum pan and heated from to 30°C at 10°C/min, at which time flowing air was introduced into the furnace at 40 mL/min and the samples were then heated to 600°C at 10°C/min. All samples (*A* to *R*) tested were extruded granulate produced via twin screw extrusion (conventional blending) used for these studies.

b) Static Stability Testing (SS)

Specimen specification:

Standard: ASTM D 2115

Shape: Sheet

Static stability tests were carried out by Teknor Apex according to the aforementioned ASTM standard. Briefly, this test involves placing samples in a convection oven at 210°C and observing the evolution of sample coloration with time, with representative samples removed every 5 minutes and the results photographed. Samples *A*, *F*, and *K* to *R* were selected for these studies.

c) Dynamic Stability Testing (DS)

Specimen specification:

Standard: ASTM D 2538

Shape: Sheet

Dynamic stability tests were carried out by Teknor Apex according to the aforementioned ASTM standard. Briefly, this test involves processing samples in a

Brabender Plasticorder and noting changes in viscosity and color with processing time at a temperature of 210°C and a screw speed of 150 rpm, using a #5 mixing bowl and with representative samples removed every 5 minutes and the results photographed. Samples *A*, *F*, and *K* to *R* were selected for these studies.

3.4.2. Mechanical Properties

a) Tensile Testing

Specimen Specification:

Standard: Modified ASTM D 882

Dimensions: Gauge length: 101.6 mm, Width: 5.97 to 6.01 mm, Thickness: 0.71 to 1 mm

Shape of the specimen: Dog bone (sheet)

Tensile tests were carried out on an Instron tensile testing machine (Model 4400). The crosshead speed was set at 50 mm/min and the gauge length was fixed at 101.6 mm. The tensile specimens were cut to the required dimensions (using a cutting die) from the extruded sheet produced using the sheet extruder for all samples *A* to *R*. Tests were carried out at room temperature (25°C), with ten specimens of each sample tested in machine direction.

b) Hardness

Specimen Specification:

Standard: Modified ASTM D 2240

Dimensions: Thickness: 3 mm

Shape of the specimen: Square (sheet)

Hardness test were carried out by using the Shore A durometer. Specimens obtained from the compression molding were used. The durometer needle was pressed into the sheet and a hardness reading was taken after 15 seconds. Testing was done at room temperature for all the samples *A* to *R*. Five readings were taken for each sample.

3.4.3. Electrical Properties

a) Volume Resistivity

Specimen Specification

Standard: Modified ASTM D 257

Dimensions: Thickness: 0.75 to 0.90 mm

Shape of the specimen: Circular (sheet)

Volume resistivity tests were carried out by using the High Resistance Meter (Hewlett Packard, Model 4329 A) and Resistivity cell (HP, Model 16008A). The specimens obtained from sheet extrusion were cut to the required dimensions by using the disk shaped cutting die. The samples were conditioned for 24 hrs at 21°C and 50% RH. Testing was performed for all samples *A* to *R*. Five readings were taken for each sample, and the thickness of each sample was measured in five different positions. Samples were placed in the instrument and 100 volts was applied to the sample for 45 seconds to measure the volume resistance of the sample. The volume resistivity was then calculated by using the formula,

$$\text{Volume Resistivity } (\Omega/\text{cm}) = 19.6 \left(\frac{\text{Resistance}}{\text{Thickness}} \right)$$

3.4.4. Fire Properties

a) Limiting Oxygen Index

Specimen Specification

Standard: ASTM D 2863

Dimensions: Length: 100 mm, Width: 6.5 mm, Thickness: 3 mm

Shape of the specimen: Rectangular (sheet)

Limiting oxygen index tests were carried out by Teknor Apex according to the aforementioned ASTM standard using strips cut from compression-molded plaques. Briefly, the strips are mounted vertically inside a testing chamber, with a mixture of nitrogen and oxygen flowing upwards through the chamber and past the sample. The sample is ignited at the top, and the oxygen content of the gas is adjusted until the sample just supports combustion, at which point the percentage of oxygen in the mix is reported.

b) Cone Calorimeter Test

Specimen Specification

Standard: ASTM E 1354 / ISO 5660

Dimensions: Length: 100 mm, Width: 100 mm, Thickness: 6.3 mm

Shape of the specimen: Square (sheet)

Cone calorimetry tests were carried out by Teknor Apex according to the aforementioned ASTM and ISO standards using square samples cut from compression-molded plaques. Briefly, the samples are mounted horizontally on a load cell (for weight measurements), heated uniformly with a set heat flux using a radiant heater, and ignited using a spark igniter. Combustion gases are drawn into a hood for analysis, and sample mass, heat output, air flow, oxygen concentration and smoke density are all measured throughout the duration of the test.

3.4.5. Plasticizer Extraction Test

Specimen Specification

Standard: Modified ASTM D 3083 (withdrawn)

Shape of the specimen: Square (sheet)

The plasticizer extraction test was performed by placing a small amount of sample in water held at a temperature of 50°C for 24 hrs. A magnetic stirrer was rotated at 300 rpm to ensure thermal uniformity. After immersion, the samples were dried at room temperature under vacuum for 6 hrs. Weights of the samples were measured before placing the samples in the water and after drying them. The plasticizer extraction was calculated by using the following formula:

$$\% \text{ Plasticizer Extraction} = 100 \left(\frac{\text{Reduction in sample mass}}{\text{Initial sample mass}} \right)$$

4. Results and Discussions

4.1. Processing

4.1.1. Dry Blending

The appearance of the dry blended samples remained the same (pale white) for all samples (*A* to *R*) regardless of the stabilizer and plasticizer used or the addition of the OMMT.

4.1.2. Melt compounding

During twin screw extrusion there was a slight increase in the torque when processing compounds containing ELO and/or OMMT (see Appendix D). The color of the pellets was observed to be identical to the control sample (*A*) for the majority of the samples processed, the exception being those samples containing non-Pb 1 stabilizer in combination with ELO plasticizer with (Sample *K*) or without (Sample *O*) OMMT or DIDP plasticizer with OMMT (Sample *G*). In these cases the color of the pellets was observed to darken. As increased coloration is generally a sign of thermal degradation in PVC (due to thermal dechlorohydration and formation of sequences of adjacent carbon-carbon double bonds), this indicates that the effectiveness of non-Pb 1 stabilizer is reduced in the presence of both ELO and the OMMT. In contrast, such qualitative observations indicate no decrease in the effectiveness of the other stabilizers under similar conditions.

4.1.3. Sheet extrusion

As with melt compounding, during the sheet extrusion, the torque was observed to increase when processing samples containing ELO and/or OMMT. Observations regarding sample coloration also were consistent with previous observations during melt compounding. The thickness of the sheets obtained is given in Appendix D.

4.2. Nanoparticle monitoring

Figure 9 shows a plot of measured nanoparticle concentrations in the size range of 5.6 to 560 nm, (1) during measurement of background concentration (10:55:06 AM) and (2) one minute later, after the weighing process for nanoclays had been initiated (10:56:06 AM) (refer to Table E-1, Appendix E, for a detailed timeline). The most significant variation between the concentrations of nanoparticles measured occurred once the weighing process was initiated, and was in the range of approximately 100 – 300 nm.

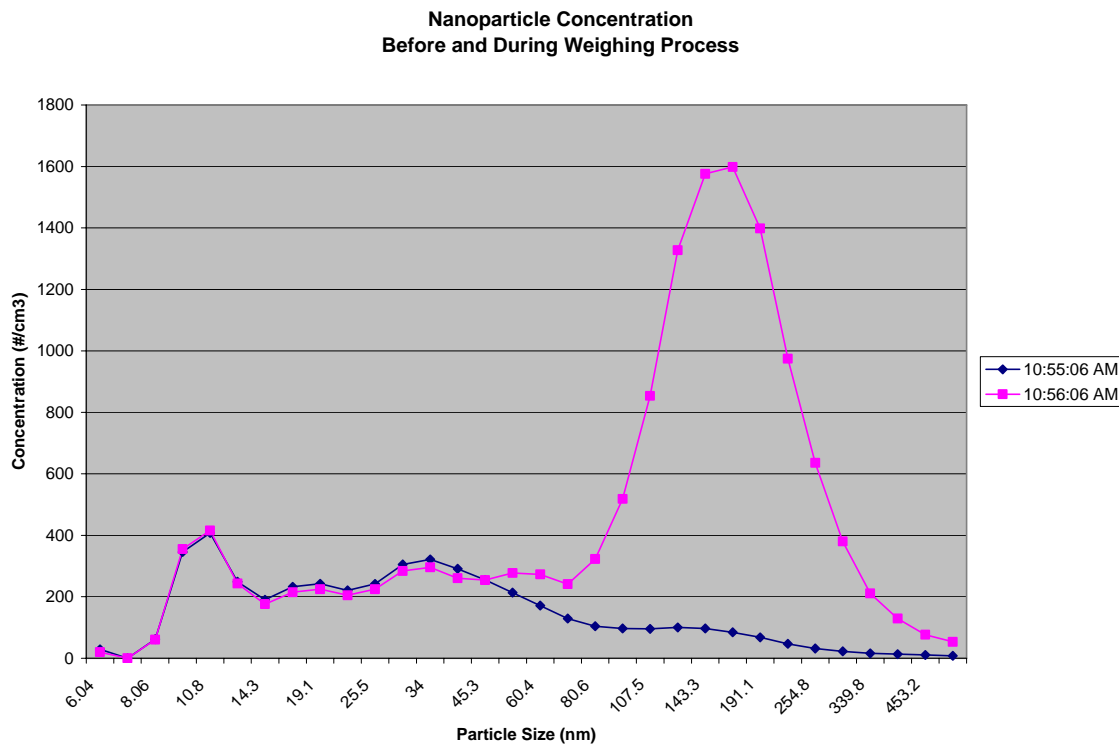


Figure 9 – Nanoparticle concentration before and during the weighing process

In particular, the particle sizes showing the greatest increase in concentration during the transition from background to the weighing process were 143.3 nm and 165.6 nm, where in both cases particle concentration increased from ~100 to ~1,600 particles/cm³. Given this result, these sizes were targeted for further study. Figure 10 shows the variation in concentrations of particles of these sizes (143.3 and 165.6 nm) over time during a typical materials handling (weighing) operation.



Figure 10 – Nanoparticle concentration during the weighing Process

The following variations in the concentration of 143.3 nm and 165.6 nm sized particles were noted during the materials handling (weighing) process:

- Background: ~100 particles/cm³
- Initiation of weighing process: Spike to ~1,600 particles/cm³
- First 7 minutes of weighing process: Gradual reduction to ~1,000 particles/cm³
- Second 7 minutes of weighing process: Constant level of ~1,000 particles/cm³

Figure 11 shows the measurement of concentrations for the various sizes of the nanoparticles from 5.6 to 560 nm at two distinct times (refer to Table E-2, Appendix E, for a detailed timeline):

1. During measurement of background concentration (11:14:06 AM)
2. After the dry blending process had been initiated (12:05:06 PM)

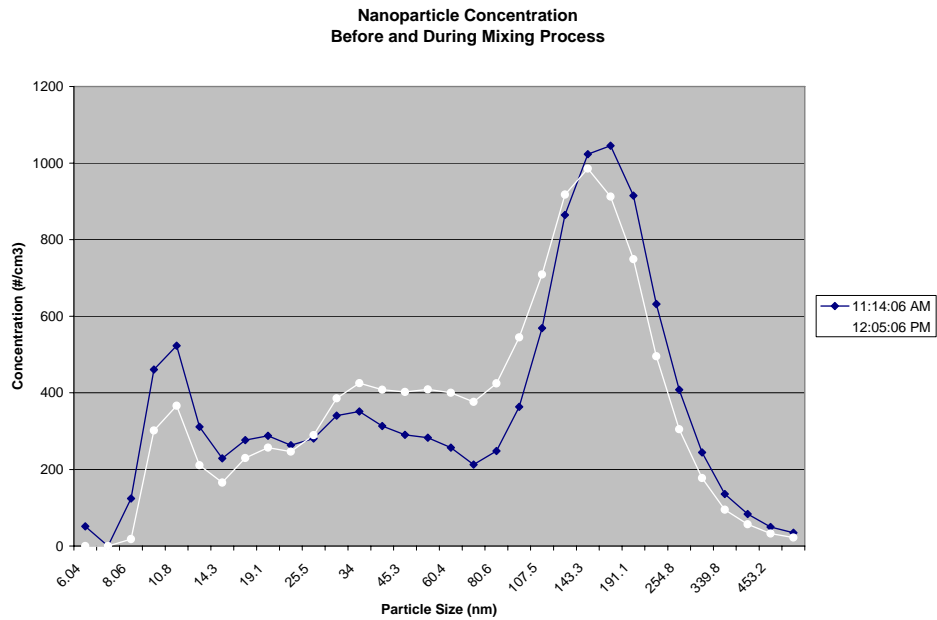


Figure 11 – Nanoparticle concentration before and during the mixing process

A similar distribution of airborne nanoparticles is detected before and during the dry blending process. The highest concentration of nanoparticles appears for particle sizes between approximately 120 to 200 nm.

Figure 12 shows two measurements taken at two different time periods.

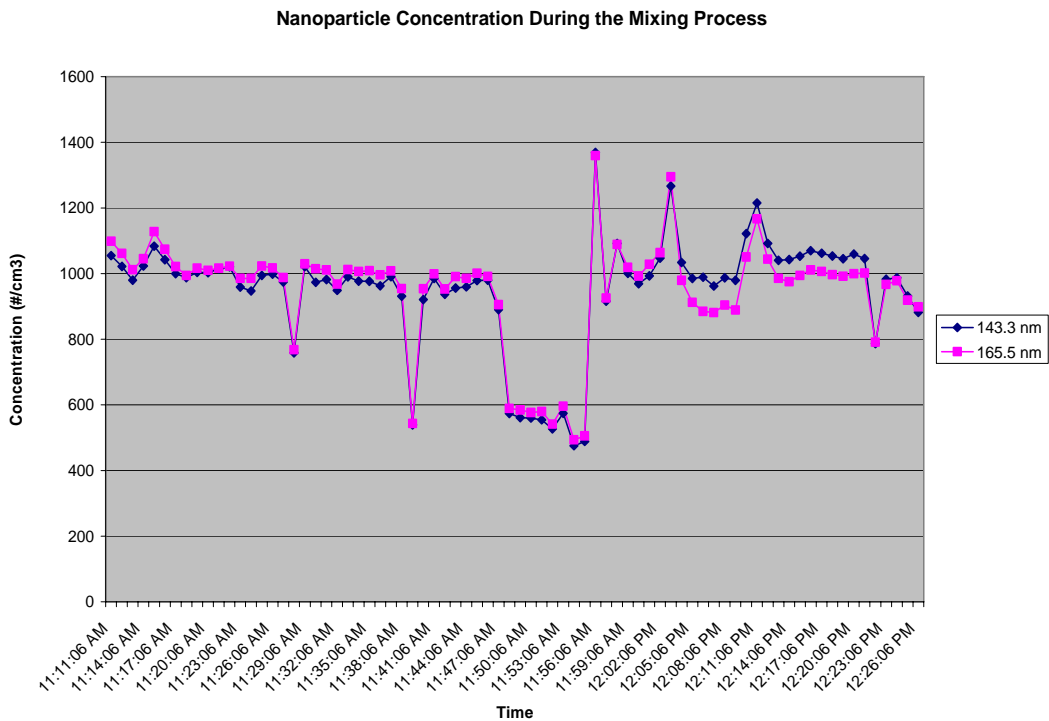


Figure 12 – Nanoparticle concentration during the mixing process

In this case the variation of nanoparticle concentration with time follows a similar pattern regardless of which of the two particle sizes is being considered. In general, the concentration remains roughly constant throughout the background measurement and mixing process at approximately 1,000 particles/cm³. This is approximately the same concentration measured at the end of the weighing process. This may be explained in one of two ways: Continuous generation of nanoparticles coupled with sufficient ventilation to reach a steady-state concentration, or, more likely, insufficient ventilation coupled with a lack of additional nanoparticles of these sizes being emitted during the dry blending process.

Figure 13 shows the measurement of concentrations for the various sizes of the nanoparticles from 5.6 to 560 nm at two distinct times (refer to Table E-3, Appendix E, for a detailed timeline):

- During measurement of background concentration (2:04:16 PM)
- After the twin screw extrusion process for nanoclays had been initiated (2:10:16 PM)

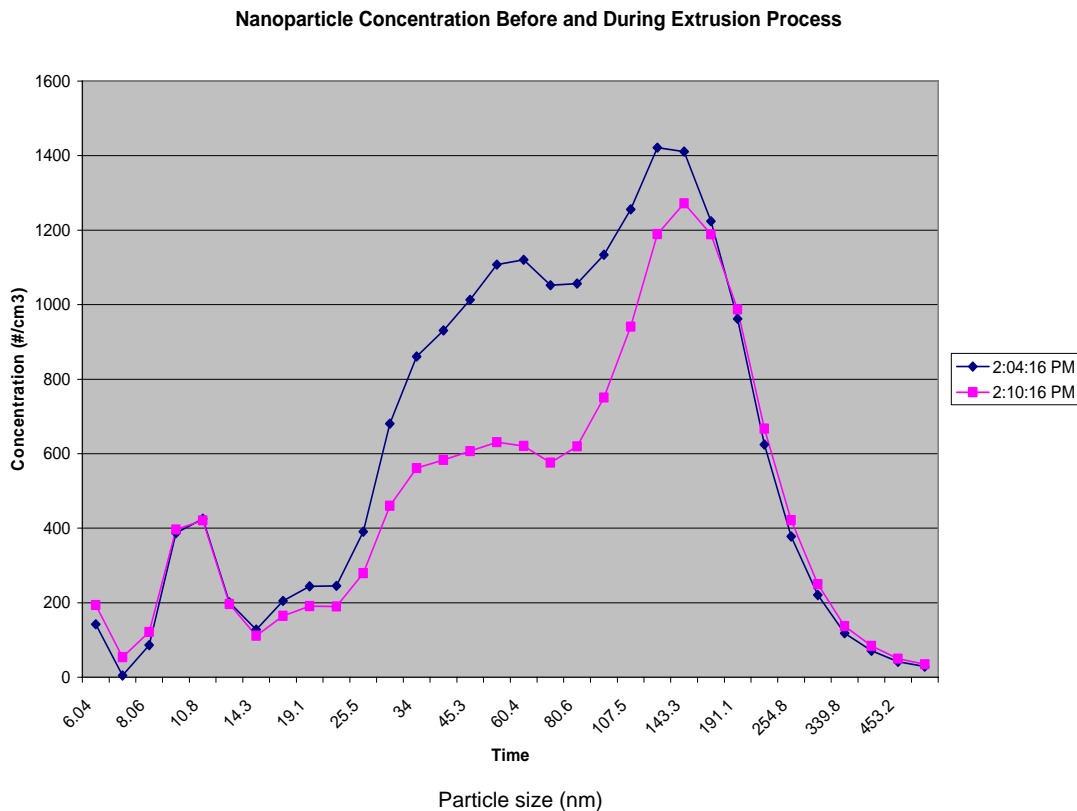


Figure 13 – Nanoparticle concentration before and during the extrusion process

Here a similar nanoparticle concentration distribution is observed before and during the twin screw extrusion process. The highest concentration of nanoparticles again appears for particle sizes between approximately 120 to 200 nm.

Figure 14 shows variations in nanoparticle concentration observed for two distinct particle sizes (143.3 nm and 165.5 nm) during the twin screw extrusion process. The spike in concentration that occurred at approximately 2:58 PM was most likely due to the operator standing on the inlet tube at that time.

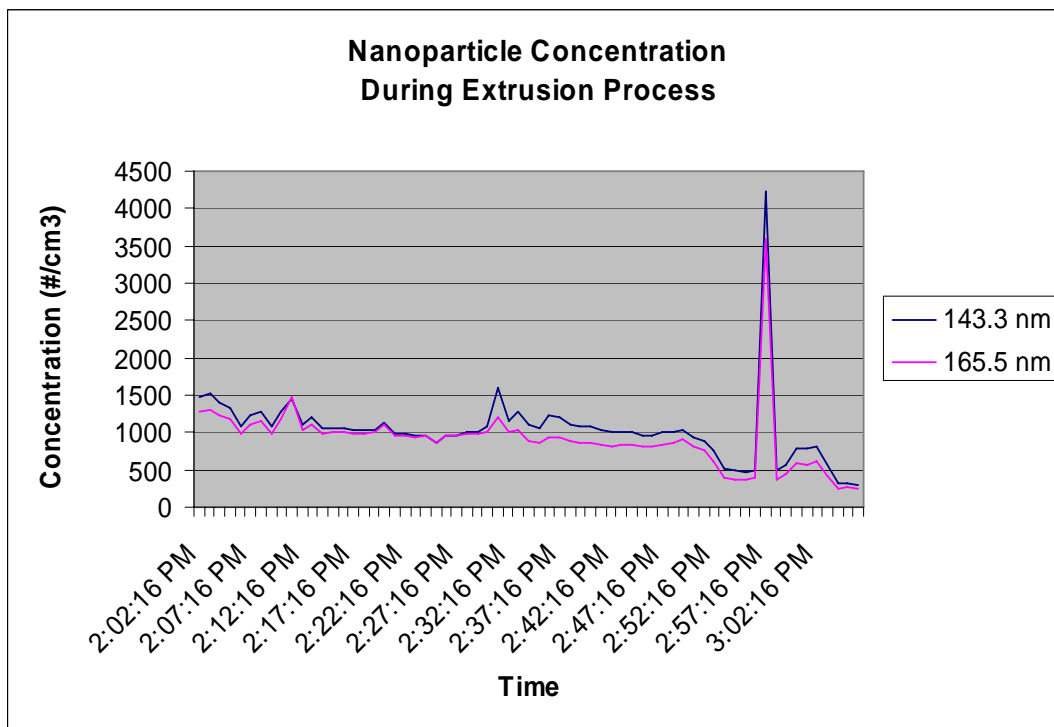


Figure 14 – Nanoparticle concentration during the extrusion process

It appears that the variations in nanoparticle concentration for both particle sizes follow a similar trend. In general, the concentration gradually decreases throughout the background measurement and extrusion process from approximately 1,500 particles/cm³ to 500 particles/cm³. This may indicate that there are no additional nanoparticles of 143.3 and 165.5 nm being emitted during the extrusion process. This may also indicate that the level of ventilation in the laboratory successfully reduces the airborne nanoparticle concentration over time.

4.3. Testing

4.3.1. Thermal Stability

a) Thermogravimetric Analysis (TGA)

Table 1 shows T_{onset} (i.e. the temperature at which the sample has lost 5% of its original mass) and T_{max} (i.e. the temperature at which the mass loss rate is at a maximum) for all the PVC compounds.

Table 1 – TGA Data for PVC and PVC / OMMT Nanocomposites

S. No.	Sample ID	T_{onset} (°C)	T_{max} (°C)
1	A	264	304
2	B	262	293
3	C	263	305
4	D	262	289
5	E	268	296
6	F	286	287
7	G	253	287
8	H	258	306
9	I	254	286
10	J	255	287
11	K	273	283
12	L	281	311
13	M	275	286
14	N	273	289
15	O	282	290
16	P	288	314
17	Q	286	291
18	R	284	285

An analysis of variance (ANOVA) of this data (excluding the lead-stabilized samples *A* and *F*) indicates that for T_{onset} statistically significant main effects exist for stabilizer type ($p = 0.012$), plasticizer type ($p = 0.000$), and nanoclay content ($p = 0.000$) (refer to Figure F-1, Appendix F). Plasticizer type was found to have the strongest effect with the average value of T_{onset} increasing from 259°C to 280°C when DIDP is replaced with ELO. The nanoclay was observed to have a lesser effect, with the average value of T_{onset} decreasing from 274°C to 265°C when 2 wt% Cloisite 30B was added to the system – consistent with the idea that the excess alkylammonium chloride modifiers present in

small quantities in the nanoclay can actually catalyze PVC degradation. Interestingly, the type of thermal stabilizer had the smallest effect on T_{onset} , with a range of average values for T_{onset} of 268°C to 273°C observed. Non-Pb 2 gave the highest average T_{onset} value, non-Pb 1 gave the lowest, and the remaining non-Pb stabilizers gave nearly the same intermediate values (269°C for non-Pb 3, 270°C for non-Pb 4).

While no statistically significant effects on T_{onset} were observed due to interactions between plasticizer and nanoclay ($p = 0.571$), small but statistically significant interactions between the stabilizer and the plasticizer ($p = 0.029$) and the stabilizer and the nanoclay ($p = 0.044$) were also observed (refer to Figure F-2, Appendix F). In particular, with respect to average T_{onset} values, non-Pb 2 stabilizer seemed to benefit more from the addition of ELO and to suffer less from the addition of 2 wt% Cloisite 30B, while non-Pb 4 showed the opposite behavior; non-Pb 1 and non-Pb 3 showed intermediate trends.

Along the same lines, the ANOVA analysis also indicates that for T_{max} a statistically significant main effect exists for stabilizer type ($p = 0.009$; refer to Figure F-3, Appendix F). In particular, the non-Pb 2 stabilizer was observed to outperform all others, giving an average T_{max} value of 309°C, vs. 289°C for the other stabilizers tested. In contrast to the effects on T_{onset} , however, it is interesting to note that no other statistically significant main effects or two-way interactions were observed ($P = 0.144$ to 0.926).

In sum, this data serves as an indication that, while all of the additives (stabilizers, plasticizer, nanoclay) play a role in setting the temperatures at which degradation begins (as indicated by interactions with T_{onset}), the process by which degradation occurs once it starts (as indicated by T_{max}) is only affected by the stabilizer. With that said, we may nevertheless conclude that ELO has a tendency to significantly delay the onset of thermal degradation upon heating, and that the nanoclay tends to degrade performance to a lesser extent. The non-Pb 2 stabilizer appears to offer the best performance of the non-lead stabilizers, giving the highest average values of both T_{onset} and T_{max} of any of the stabilizers, and remains the only additive studied here that produced a statistically significant change in T_{max} .

Finally, in terms of overall system performance, the four lead- and phthalate-free nanocomposite systems (samples *K* to *N*) all show higher T_{onset} values than the lead-

stabilized control (sample *A*), with one of the four (sample *L*) also showing superior performance versus the lead-stabilized control with respect to T_{\max} . Analogous systems without nanoclay show similar performance levels, with samples *O* to *R* outperforming sample *A* with respect to T_{onset} and sample *P* showing a superior value of T_{\max} as well. While the improvements are by no means huge, and we do not see strong evidence of stabilizer / nanoclay synergy in the data, this validates the idea that, as measured by TGA in air, it is possible to formulate lead- and phthalate-free systems with higher T_{onset} and T_{\max} values indicative of improved thermal stability in the context of the TGA experiment.

b) Static and Dynamics Stability Testing (SS / DS)

Table 2 shows the results of static and dynamic stability testing of selected samples. The sample number refers to the photographic images of actual test samples taken at five minute intervals during these tests, shown in Figure 15 (SS) and Figure 16 (DS).

Table 2 – Static and dynamic heat stability results for PVC and selected PVC / OMMT Nanocomposites

No.	Sample	Time to failure	
		Static stability (210 °C)	Dynamic stability (210 °C, 150 rpm)
1	A	20	48
2	O	10	43
3	P	25	27
4	Q	15	78
5	R	20	69
6	K	10	9
7	L	20	18
8	M	10	10
9	N	15	6
10	F	15	33

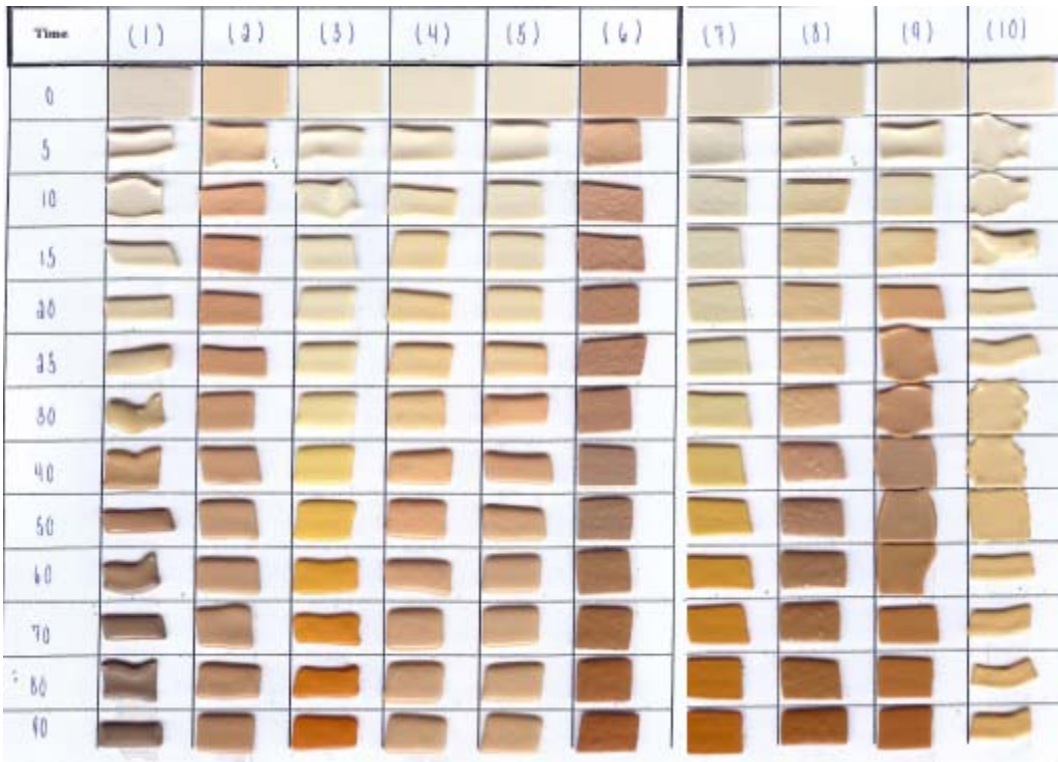


Figure 15 – Static heat stability test specimens, tested in an oven at 210 °C and removed at 5 minute intervals (time in left-hand column indicated in minutes).

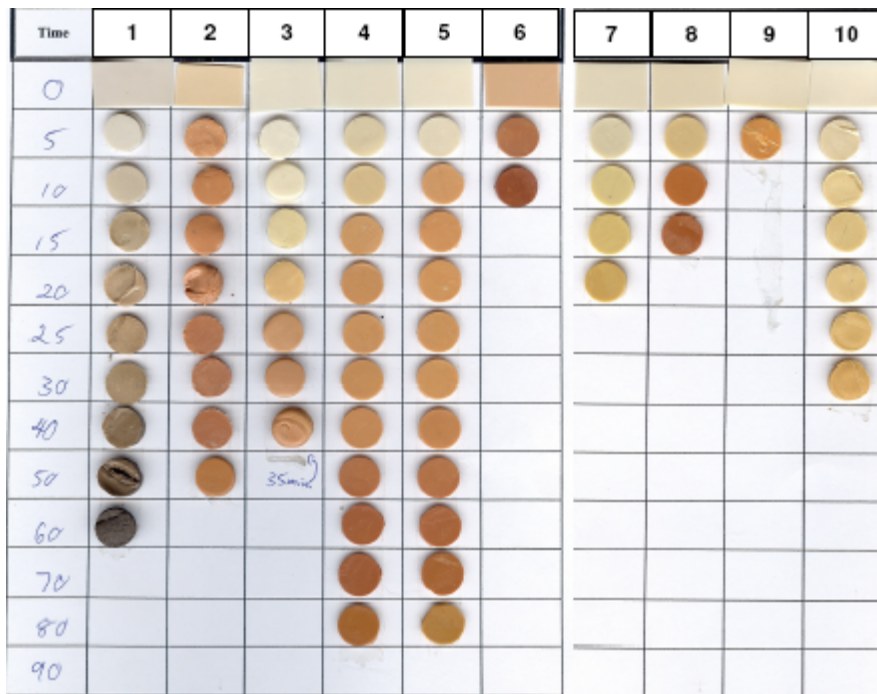


Figure 16 – Dynamic heat stability test specimens, tested in a torque rheometer at 210 °C and 150 rpm and removed at 5 minute intervals (time in left-hand column indicated in minutes).

As the static stability data is somewhat subjective in nature, an ANOVA was not performed. With that said, an overview of the data indicates several trends. First, the replacement of DIDP by ELO in a lead-stabilized system results in a slight decrease in static stability, with color failure occurring at 15 minutes with ELO vs. 20 minutes with DIDP. It is clear, however, that the performance of the nanoclay-free ELO-based systems is highly stabilizer dependent, with systems based on non-lead stabilizers showing color failure in anywhere from 10 to 25 minutes depending on the stabilizer. Non-Pb 2 gave the best results (25 minutes), followed by non-Pb 4 (20 minutes), non-Pb 3 (15 minutes), and non-Pb 1 (10 minutes, with unacceptable initial color). When nanoclay is added to these systems, the same relative order of stability is observed versus non-lead stabilizer type, but with a 5 minute reduction in time to color failure in all but the non-Pb 1 based sample, which again showed poor initial color. It seems, therefore, that plasticizer/stabilizer interactions tend to be very specific as far as the results of static stability testing are concerned, and that nanoclay tends to degrade performance in this test. Nevertheless, the data also demonstrate that color and static stability on par with the lead-stabilized, DIDP plasticized control can be achieved in a lead-free, ELO plasticized nanocomposite.

An ANOVA (excluding the lead-stabilized samples *A* and *F*) was performed on the dynamic stability data, but due to the sparse dataset and lack of replicates, the results were less conclusive. The primary result, as above, is that the addition of nanoclay tended to significantly reduce time to failure from an average of 54.25 minutes to an average of 10.75 minutes regardless of stabilizer type ($p = 0.051$). Qualitatively, the effect of stabilizer type is also obvious, but system-specific, and does not correlate well with the dynamic stability tests. The lubricating stabilizers both gave exceptionally good dynamic stability in combination with ELO, with failure occurring at times nearly double that of the lead-stabilized, DIDP-plasticized control. The non-Pb 1/ELO system produced results more or less on par with the aforementioned control, and the non-Pb 2/ELO system gave the earliest time to failure, a paradoxical result given its excellent performance in the static stability tests. It is also interesting to note here that the addition of the nanoclay effectively reduces the three highest performing systems to a rather minimal level of performance, with failure in ~10 minutes or less. The exception is the non-Pb 2/ELO system, which experiences a much more modest reduction in dynamic stability upon

addition of the nanoclay, transforming this system from the least stable in its absence to the most stable in its presence, at least in the context of this test.

These results serve to highlight the complex inter-additive interactions present in these systems. Along the same lines, it is also noted that the replacement of DIDP by ELO in the lead-stabilized systems studied here actually resulted in a decrease in dynamic stability, in spite of the much higher dynamic stabilities achieved via the combination of ELO with compatible non-lead stabilizers. The ANOVA results are shown in Appendix H, though it should be noted that only the effect of the nanoclay was indicated to be statistically significant. In spite of this, it is again observed that plasticizer/stabilizer interactions tend to be very specific as far as the results of static stability testing are concerned, and that nanoclay tends to degrade performance in this test. In this case, however, as opposed to the case of static stability, where parity was achieved, the best lead-free ELO plasticized nanocomposite is still inferior to the lead-stabilized, DIDP-plasticized control.

In sum, the static and dynamic stability tests indicate that, while the lead-free ELO-plasticized nanocomposites can pass an initial color stability test and can match the lead-stabilized, DIDP-plasticized control with respect to static stability, that this is not possible in the case of dynamic stability and that the addition of the nanoclay has a detrimental effect on stability in general. This may however be ascribed to the presence of excess modifier, as noted previously, meaning that this issue seems to be neither inherent nor insurmountable. Additionally, it is also shown that the combination of ELO and compatible non-lead stabilizers can give substantial improvements in dynamic stability vs. the lead-stabilized, DIDP-plasticized control, confirming the utility of such a combination with respect to practical thermal stability.

4.3.2. Mechanical Properties

a) Tensile Properties

Table 3 shows the tensile properties obtained for the PVC compounds.

Table 3 – Tensile Data for PVC and PVC / OMMT Nanocomposites

S. No.	Sample	Tensile Stress at Break (MPa)		Tensile Strain at Break (%)		100% Modulus (MPa)	
		Avg	S.D	Avg	S.D	Avg	S.D
1	A	22.3	0.9	181	10	17.0	0.3
2	B	19.7	0.6	182	11	15.4	0.4
3	C	23.6	0.2	129	4	20.8	0.3
4	D	20.6	0.7	195	3	14.6	0.7
5	E	23.9	1.0	196	3	16.9	0.8
6	F	25.1	1.1	178	4	20.3	0.9
7	G	17.8	3.9	95	15	22.5	-
8	H	23.8	0.1	162	0	18.9	0.1
9	I	21.0	0.8	173	31	17.1	0.5
10	J	19.2	0.5	158	7	16.4	0.4
11	K	25.5	1.0	142	5	23.0	1.0
12	L	25.0	0.9	176	5	18.9	1.2
13	M	24.6	0.6	148	5	21.6	0.7
14	N	23.9	0.9	175	8	19.3	1.6
15	O	24.1	0.3	183	3	18.0	0.1
16	P	24.6	0.5	227	2	14.5	0.7
17	Q	26.8	0.4	199	6	17.5	0.7
18	R	27.2	0.9	193	2	18.4	0.5

An ANOVA of this data (excluding the lead-stabilized samples *A* and *F*) indicates that statistically significant main effects exist between all three measures of mechanical properties (break stress, break strain, and stress at 100% strain, a.k.a. 100% modulus) and stabilizer type, plasticizer type, and nanoclay content ($p = 0.000$ in all cases).

In terms of break stress (refer to Figure G-1, Appendix G), plasticizer type has by far the largest impact, with the replacement of DIDP by ELO resulting in an increase in average break stress from 21.1 to 25.3 MPa (+20%). Stabilizer type has the next most significant effect, with non-Pb 2 giving the highest average break stress value (24.1 MPa), non-Pb 1 giving the lowest (21.5 MPa), and the lubricating stabilizers giving intermediate values (23.4 MPa for non-Pb 3, 23.7 MPa for non-Pb 4). Finally, the addition of 2 wt% of Cloisite 30B was observed to give a small reduction in the average break stress value, from 23.9 MPa to 22.5 MPa (-6%). As a point of interest, it is notable that these trends in break stress track quite closely with the main effects observed in the ANOVA analysis of T_{onset} ; the reason for this is not known.

While no statistically significant effects on break stress were observed due to interactions between plasticizer and nanoclay ($p = 0.125$), statistically significant

interactions between the stabilizer and the plasticizer and the stabilizer and the nanoclay ($p = 0.000$ in both cases) were observed (refer to Figure G-2, Appendix G). In particular, with respect to average break stress values, the non-Pb 2 stabilizer seemed to benefit the least from the addition of ELO but was the only one to show no change in break stress upon addition of 2 wt% Cloisite 30B. In contrast, non-Pb 1 stabilizer benefited the most from the addition of ELO, with the lubricating stabilizers showing similar, intermediate trends. Likewise, non-Pb 4 experienced a significant degradation in performance upon addition of 2 wt% Cloisite 30B, whereas the non-Pb 1 and non-Pb 3 stabilizers showed similar, smaller reductions in break stress in combination with the nanoclay. Finally, the three way interaction of plasticizer, stabilizer, and nanoclay is also statistically significant ($p = 0.000$), with the ELO/non-Pb 4/0 wt% Cloisite 30B system (sample *R*) giving the highest break stress (27.2 MPa) of any of the samples.

With respect to break strain (refer to Figure G-3, Appendix G), of the three individual factors we find that the presence or absence of nanoclay has the largest effect – when 2 wt% Cloisite 30B is added, the average break strain drops from 187% to 154% (a decrease of 18%). The effect of the stabilizer is nearly as significant in magnitude, however, with non-Pb 1 giving an average break strain of 148%, far lower than non-Pb 2 (173%), non-Pb 3 (182%) or non-Pb 4 (180%). Interestingly, the effect of plasticizer, while still quite large, is the smallest of the three, with the replacement of DIDP by ELO resulting in an increase in average break strain from 162% to 180% (an increase of 11%).

In terms of two-way interactions (refer to Figure G-4, Appendix G), all were found to be statistically significant ($p = 0.000$). Of the two-way interactions, the combined effect of stabilizer and plasticizer on break strain was the largest, with the non-Pb 2 stabilizer showing the greatest benefit upon replacement of DIDP by ELO. Non-Pb 1 shows a similar trend of slightly smaller magnitude, while non-Pb 4 shows almost no preference for ELO over DIDP (only a slight increase in break strain), and non-Pb 3 shows an aversion to ELO, displaying a small decrease in break strain. The stabilizer/nanoclay interaction had the next largest effect, with the non-Pb 1 stabilizer suffering the greatest loss in break strain in response to the addition of 2 wt% Cloisite 30B. The two lubricating stabilizers behave effectively identically, showing less sensitivity to the addition of the nanoclay (though a significant loss in break strain nevertheless occurs). Finally, non-Pb 2 shows the least sensitivity, exhibiting only a small

loss in break strain upon addition of nanoclay. The plasticizer / nanoclay interaction is the smallest in magnitude, though it is nevertheless observed that ELO shows a somewhat greater sensitivity to the addition of nanoclay (evidenced by a slightly larger loss in break strain) than DIDP. Finally, the three way interaction of plasticizer, stabilizer, and nanoclay is also statistically significant ($p = 0.000$), with the ELO/non-Pb 2/0 wt% Cloisite 30B system (sample *P*) giving the highest break strain (227%) of any of the samples, and the only value above 200%.

Lastly, with respect to 100% modulus (stress at 100% strain), of the individual factors (refer to Figure G-5, Appendix G) the most important is the presence of the nanoclay, with the addition of 2 wt% Cloisite 30B increasing the average 100% modulus from 17.0 MPa to 19.7 MPa (an increase of 16%). The effect of the stabilizer is the next most significant, with the higher values coming from the non-lubricating stabilizers (19.8 MPa for non-Pb 1, 18.2 MPa for non-Pb 2) and the lower values coming from the lubricating stabilizers (17.9 MPa for non-Pb 3, 17.6 MPa for non-Pb 4). Finally, the effect of the plasticizer is fairly small, with the replacement of DIDP by ELO resulting in a modest increase in average 100% modulus from 17.9 MPa to 18.8 MPa (an increase of 6%).

As with the break strain, all two-way interactions (refer to Figure G-6, Appendix G) were found to be significant in the case of average 100% modulus as well ($p = 0.000$). The stabilizer/plasticizer interaction was the strongest, with non-Pb 3 showing the greatest increase in average 100% modulus upon replacement of DIDP by ELO. The non-Pb 1 and non-Pb 4 stabilizers showed similar but somewhat smaller increases as well, while non-Pb 2 actually showed a significant *decrease* in average 100% modulus when DIDP was replaced with ELO. The stabilizer / nanoclay interaction was almost as strong, with non-Pb 1 showing by far the largest increase in response to the addition of nanoclay, versus a much smaller increase observed with non-Pb 3 stabilizer and the similar and slightly smaller increase observed with non-Pb 2. In contrast, the average 100% modulus of systems based on non-Pb 4 was more or less unaffected by the addition of the Cloisite 30B. The plasticizer/nanoclay interaction was much weaker than the two aforementioned interactions, with somewhat more stiffening observed in ELO-based systems than in DIDP-based systems upon addition of the nanoclay – consistent with prior arguments that ELO will interact more strongly with Cloisite 30B than DIDP. Finally, the three way

interaction of plasticizer, stabilizer, and nanoclay is also statistically significant ($p = 0.000$), with the ELO/non-Pb 1/2 wt% Cloisite 30B system (sample *K*) giving the highest 100% modulus (23 MPa) of any of the samples.

From these results we can see that the replacement of DIDP by ELO results, in general, in increases in all three mechanical properties measured, with increases in break stress being the most significant versus lesser increases in break strain and 100% modulus. In contrast, the addition of the nanoclay tends to slightly reduce break stress and more significantly reduce break strain, while giving modest increases in 100% modulus. What is also apparent here, however, and somewhat surprising as well, is the role of stabilizer in altering the mechanical properties of the formulation. In terms of maximizing ultimate properties without overly stiffening the material, non-Pb 2 stabilizer appears to have some advantages, giving the highest break stress and good break strain values in general while showing the least sensitivity to the detrimental effects caused by the addition of nanoclay coupled with a strong tendency to produce compliant, ductile samples (i.e. with high break strains and low 100% moduli) in combination with ELO.

Finally, completing our discussion through a comparison of the aforementioned data with our lead stabilized, DIDP plasticized control (sample *A*), we find that it is possible to effectively match, to within $\sim 10\%$, all of the mechanical properties of the control system. Lead- and phthalate-free nanocomposites (samples *L* and *N*) can be made to give values of break stress, break strain, and secant modulus quite similar to those found in the control, while some of the analogous nanoclay-free systems (samples *O*, *Q* and *R*) actually outperform the control across the board, showing a combination of greater strength, ductility, and stiffness, meaning substantially higher elongational toughness as a result. So far, then, the lead- and phthalate-free sample *P* and its nanocomposite equivalent, sample *L*, lead the pack with their ability to match or surpass the lead stabilized, phthalate plasticized control with respect to both thermal properties (as measured by TGA in air) and mechanical properties (as measured by tensile testing).

b) Hardness

Table 4 shows the hardness data obtained for all the PVC and PVC / OMMT compounds.

Table 4 – Hardness Data for PVC and PVC/OMMT Nanocomposites

S. No.	Sample ID	Hardness (Shore A)		
		Average	Std. dev	Std.error
1	A	83.6	0.5	0.2
2	B	76.4	0.5	0.2
3	C	79.2	0.8	0.4
4	D	82.2	0.4	0.2
5	E	84	0.7	0.3
6	F	84.8	0.4	0.2
7	G	78.4	0.5	0.2
8	H	80.4	0.5	0.2
9	I	84.8	0.4	0.2
10	J	86.2	0.4	0.2
11	K	82.6	0.5	0.2
12	L	81	0.6	0.3
13	M	84.4	0.4	0.2
14	N	84.3	0.4	0.2
15	O	81.3	0.4	0.2
16	P	79.4	0.5	0.2
17	Q	78	0.7	0.3
18	R	79.3	0.4	0.2

For hardness testing results, an ANOVA of this data (excluding the lead-stabilized samples *A* and *F*) indicates that statistically significant main effects exist for stabilizer type and nanoclay content ($p = 0.000$ in all cases; refer to Figure G-7, Appendix G). The plasticizer main effect, on the other hand, is not statistically significant ($p = 0.325$). Of the significant interactions, the stabilizer interaction is somewhat stronger, with the average Shore A hardness increasing from 79.7 MPa to 80.0 MPa to 82.4 MPa to 83.5 MPa when moving from non-Pb 1 to non-Pb 2 to non-Pb 3 to non-Pb 4. The effect of the nanoclay is almost as large, with the addition of 2 wt% Cloisite 30B resulting in an increase in average Shore A hardness from 80.0 MPa to 82.8 MPa (an increase of 4%).

In terms of two-way interactions (refer to Figure G-8, Appendix G), all three are significant ($p = 0.000$), but the stabilizer / plasticizer interaction is by far the strongest. In this case non-Pb 1 shows a substantial increase in average Shore A hardness when moving from DIDP to ELO, versus non-Pb 2, which shows almost no change, and the lubricating stabilizers, which show similarly significant decreases. The stabilizer/nanoclay interaction is the next strongest, with the lubricating stabilizers (non-Pb 3 and non-Pb 4) showing a greater increase in hardness upon addition of 2 wt% Cloisite 30B

than the non-lubricating stabilizers (non-Pb 1 and non-Pb 2). Finally, the plasticizer/nanoclay interaction is such that a greater increase in hardness is observed when adding 2 wt% Cloisite 30B to an ELO plasticized system than to a DIDP plasticized system – again reinforcing the idea that the ELO and the Cloisite 30B do indeed show some added affinity for one another.

Finally, in terms of performance comparisons, we see that all of the lead and phthalate free formulations give hardness values within ~7% of that of the lead stabilized, DIDP plasticized control (sample *A*). Furthermore, the lead and phthalate free nanocomposites in particular (samples *K* through *N*) give hardness values almost identical to the aforementioned control sample. We therefore conclude that none of the alternative formulations would be unacceptable for reasons of hardness.

4.3.3. Electrical Properties

a) Volume Resistivity

Table 5 shows the volume resistivity data obtained for all the PVC and PVC/OMMT compounds.

Table 5 – Volume Resistivity Data for PVC and PVC/OMMT Nanocomposites

S. No.	Sample	Volume resistivity (Ω/cm)		
		Average	Std. dev	Std. error
1	A	1.5×10^{15}	0.3×10^{15}	0.2×10^{15}
2	B	2.0×10^{15}	0.4×10^{15}	0.2×10^{15}
3	C	5.2×10^{11}	0.7×10^{11}	0.3×10^{11}
4	D	7.4×10^{14}	0.7×10^{14}	0.3×10^{14}
5	E	7.0×10^{14}	0.7×10^{14}	0.3×10^{14}
6	F	4.7×10^{15}	1.4×10^{15}	0.6×10^{15}
7	G	1.4×10^{13}	0.03×10^{13}	0.01×10^{13}
8	H	2.8×10^{11}	0.05×10^{11}	0.02×10^{11}
9	I	8.2×10^{12}	0.3×10^{12}	0.1×10^{12}
10	J	1.2×10^{13}	0.02×10^{13}	0.01×10^{13}
11	K	1.1×10^{14}	0.02×10^{14}	0.01×10^{14}
12	L	2.5×10^{12}	0.1×10^{12}	0.05×10^{12}
13	M	9.0×10^{13}	0.09×10^{13}	0.04×10^{13}
14	N	2.5×10^{13}	0.06×10^{13}	0.03×10^{13}
15	O	6.7×10^{14}	0.1×10^{14}	0.04×10^{14}
16	P	6.8×10^{11}	0.4×10^{11}	0.2×10^{11}
17	Q	5.0×10^{14}	0.2×10^{14}	0.08×10^{14}
18	R	4.3×10^{14}	0.1×10^{14}	0.05×10^{14}

The ANOVA of this data (excluding the lead-stabilized samples *A* and *F*), performed originally without any additional treatment, failed to pass the normality tests when considering three-way interactions. As such, ANOVA was performed instead on the \log_{10} of the volume resistivity values measured for these samples, which allowed the data set to pass the normality tests for three-way interactions. Because of significant variations in the trends noted between the two ANOVAs, however, some uncertainties exist with respect to the interpretation of the statistical data.

With that in mind, we simply report that, for ANOVA of volume resistivity, all main effects and two way interactions appear to be statistically significant ($p = 0.000$ in both ANOVAs; refer to Figures I-1 and I-2, Appendix I), and that the stabilizer and the nanoclay seem to have a greater impact on volume resistivity than the plasticizer. Three way interactions are also statistically significant in this system, with the non-Pb 1/DIDP/0 wt% Cloisite 30B formulation (sample *B*) showing the highest volume resistivity (2×10^{15}) of any lead-free formulation.

We can nevertheless discuss the qualitative effects observed by simply examining the data reported in Table 5. In terms of OMMT-free systems, one significant observation is that the volume resistivity (VR) of sample *F* (ELO + Pb) is almost three times greater

than that of sample *A* (DIDP + Pb). Comparisons of the lead-free DIDP (*B* to *E*) and ELO (*O* to *R*) based systems, however, show smaller changes in VR and tend to favor a slight decrease in VR when DIDP is replaced with ELO. While the difficulties associated with accurately measuring such high values of VR makes interpretation of smaller differences difficult, these trends do suggest that ELO can improve VR, but only in combination with certain thermal stabilizers.

Likewise, while the VR of the sample containing non-Pb 1 stabilizer and DIDP (*B*) is almost twice that of the control sample (*A*), the same stabilizer in combination with ELO (*O*) gives a two-fold *decrease* in VR versus the ELO control (*F*), and the other lead-free stabilizers all give lower values of VR versus their respective controls (*C* to *E* vs. *A*, *P* to *R* vs. *F*). These results indicate that the use of lead-free stabilizers generally tend to lower VR – substantially in some cases, with non-Pb 2 reducing VR by more than three orders of magnitude vs. the lead-stabilized control regardless of plasticizer type.

With respect to the PVC/OMMT nanocomposite systems, the volume resistivity of the DIDP-plasticized, non-lead stabilized samples (*G* to *J*) is reduced across the board through the addition of OMMT, with the severity of the reduction observed to be greater in those samples with a higher value of VR in the absence of OMMT. This can be rationalized by the fact that the OMMT contains a small amount (~1-2 wt%) of free quaternary ammonium salt that acts as a mobile ionic impurity. With that said, in ELO-plasticized systems, OMMT-containing samples (*K* to *N*) compare more favorably with their OMMT-free counterparts (*O* to *R*), with an increase in VR observed in the sample containing non-Pb 2 stabilizer with (*L*) versus without (*P*) OMMT, and smaller decreases in the other samples versus the case in the DIDP plasticized systems. This observation is consistent with the existence of favorable interactions between the ELO and the clay modifiers present in the OMMT, with the ability of the ELO to sequester free quaternary ammonium salts expected to mitigate the drop in VR that would otherwise be seen in their presence. Interestingly, less variability in resistivity is seen in those samples containing OMMT. This may be due to the larger errors associated with measuring higher VR values, but this explanation cannot fully explain the data, given the extremely low errors reported for both high VR (*K*) and much lower VR (*H*) nanocomposite systems. Such results imply a high degree of homogeneity in the nanocomposite samples as well.

While it is unfortunate to note that non-Pb 2 stabilizer, which showed such excellent thermal and mechanical performance, gives extremely poor VR values, overall these results show that the lead-free, ELO stabilized nanocomposite systems display VR values superior to their DIDP plasticized counterparts and in the range of the lead- and OMMT-free, DIDP plasticized systems. While this level of performance falls short of our lead stabilized, phthalate plasticized control (sample *A*), it is nevertheless well within the usable range for vinyl wire and cable insulation, and could be further improved if extra care were taken to remove all free quaternary ammonium salts from the OMMT. In particular, among the lead and phthalate free nanocomposites, samples *K* and *M* give VR values on the order of $\sim 1 \times 10^{14} \Omega/\text{cm}$, while lead- and phthalate-free non-nanocomposite formulations (samples *O*, *Q*, and *R*) give VR values on the order of $\sim 5 \times 10^{14} \Omega/\text{cm}$. This is significant because the typical range of VR values found in wire and cable insulation are $1\text{-}5 \times 10^{14} \Omega/\text{cm}$ ⁶⁷. Therefore, while these systems do not match the lead stabilized, DIDP plasticized control with respect to VR values, they nevertheless give performance good enough for use in wire and cable applications.

4.3.4. Fire Properties

Table 6 shows the results of cone calorimetry (in the form of peak heat release rate, PHRR) and limiting oxygen index (LOI) testing of selected samples.

Table 6 – Fire Properties Data for PVC and PVC/OMMT Nanocomposites

Sample	Peak heat release rate (kW/m ²)	Limiting oxygen index (%)
A	270	28.5
F	330	29.5
K	250	33
L	250	29
M	270	33
N	310	31.5
O	300	31
P	330	28.5
Q	320	29.5
R	300	31.5

An ANOVA (excluding the lead-stabilized samples *A* and *F*) was performed on the PHRR and LOI data (results shown in Appendix J), but as in the case of the dynamic

stability data, due to the sparse dataset and lack of replicates, the results were less conclusive, and none of the main effects were considered statistically significant at a 95% confidence level.

With that said, the strongest effects all related to the presence of the nanoclay. In particular, the addition of 2 wt% nanoclay was observed to reduce PHRR by an average of 13% ($p = 0.278$), with noticeable reductions seen in all lead-free ELO-plasticized systems except in the case of non-Pb 4. The overall trend is consistent with previous discussions regarding the ability of nanoclays to improve fire retardance. This is a very positive development given that one drawback of the replacement of DIDP by ELO in the lead-stabilized control system is an 11% increase in PHRR. The nanoclay shows itself to be very complimentary to the ELO in this regard by more than compensating for this effect, to the point where three out of four of the lead-free ELO-plasticized nanocomposites show similar (non-Pb 3) or lower (non-Pb 1 and non-Pb 2) PHRR values versus the lead-stabilized, DIDP-plasticized control.

Along the same lines, analysis of the limiting oxygen index (LOI) data indicates an increase in average LOI from 30.13% to 31.63% with the addition of 2 wt% nanoclay ($p = 0.154$). Interestingly, the only system not to benefit from the nanoclay in this regard is again based on non-Pb 4, indicating that this stabilizer is not particularly compatible with the ELO/nanoclay combination when it comes to fire properties. Stabilizer choice is also significant ($p = 0.173$), with non-Pb 2 showing the worst performance of all of the non-lead stabilizers. Finally, plasticizer choice appears to matter as well; in contrast to PHRR, where ELO results in degraded fire performance, in the case of LOI the replacement of DIDP by ELO in a lead-stabilized system results in an increase in LOI from 28.5% to 31.5%. Putting these effects together, every one of the lead-free, ELO-plasticized nanocomposite systems outperforms the lead-stabilized, DIDP-plasticized control; in fact, the aforementioned control sample is actually the worst performer of all samples analyzed.

In sum, then, the combination of ELO and nanoclay is advantageous in that it erases the potential disadvantage of increased PHRR associated with replacing DIDP with ELO. The end result is that three out of four lead-free, ELO-plasticized nanocomposite systems match or best the lead-stabilized, DIDP-plasticized control with

respect to both PHRR and LOI, and all four show an advantage in at least one of the two metrics.

4.3.5. Plasticizer Extraction Test

The extractable fractions measured for sample *A* (DIDP plasticized) and sample *F* (ELO plasticized) were 0.027 wt% and 0.037 wt%, respectively – a roughly equivalent result given the experimental error associated with measuring such small changes in mass, the possibility for changes in water uptake as a result of differences in plasticizer type, and the fact the ASTM standard used has since been withdrawn.

5. Conclusions

Lead- and phthalate- free PVC/nanoclay nanocomposites have been successfully prepared by the melt blending of PVC with organically modified nanoclay. Data taken during the various processing steps indicate that these materials process in a similar fashion to their conventional counterparts, with greater torque observed during extrusion processing but without the need to adjust the process parameters substantially to ensure proper materials production.

TGA analyses indicate that the alternative lead and phthalate free formulations show higher values of T_{onset} versus the lead stabilized, phthalate plasticized control system – evidence of the stabilizing effects of ELO on these PVC formulations. Some also surpass the control with respect to T_{max} values as well, thanks to the excellent performance of non-Pb 2 stabilizer. With that said, static and dynamic stability tests show that TGA results are unable to fully capture the thermal stability of these materials under more realistic conditions, and that while the lead free, ELO plasticized systems can outperform the lead stabilized, phthalate plasticized controls with respect to both static and dynamic stability, the addition of the nanoclay erases these improvements with respect to static stability and more than counteracts them with respect to dynamic stability. Still, this is consistent with the reduction in T_{onset} observed when adding nanoclay to lead free, ELO plasticized formulations. Furthermore, non-Pb 2 stabilizer is again observed to be a stand-out in these systems in terms of performance, giving similar

static stability and approaching the dynamic stability of the lead stabilized, phthalate plasticized control.

Tensile testing indicates that the addition of nanoclay slightly reduces the break stress and more significantly reduces the break strain, while increasing the 100% modulus – resulting in a stiffer, less ductile material. However, replacement of DIDP by ELO tends to result in substantial increases in break stress as well as additional increases in break strain and 100% modulus, making ELO plasticized materials substantially tougher than their DIDP plasticized counterparts and helping to balance the changes induced by the introduction of the nanoclay. Stabilizer type was also found to have a significant effect on mechanical properties, and non-Pb 2 stabilizer again shows excellent performance here as well. Overall, we find that it is possible to match or improve upon the mechanical properties of the control using lead- and phthalate-free formulations. The same holds true with respect to hardness measurements, where all lead- and phthalate-free samples give hardness values very close to those of the control and the nanocomposite systems in particular match the hardness of the control formulation almost exactly.

Volume resistivity studies indicate that the addition of nanoclay tends to substantially decrease the resistivity of DIDP-plasticized formulations, but that this effect is mitigated by the replacement of DIDP with ELO, and can even be reversed in the presence of the non-Pb 2 stabilizer, indicative of more favorable interactions between the ELO and the OMMT than between the DIDP and the OMMT. ELO content also tends to increase volume resistivity, though this effect is inconsistent and seems to depend on stabilizer type. Overall, lead-free ELO-plasticized nanocomposite systems give resistivities acceptable for use in wire and cable applications, and show much less variation in resistivity versus OMMT-free systems. Along these lines, extractability tests also give acceptable results, indicating no major changes in performance when replacing DIDP with ELO.

Finally, with respect to fire properties, while it is observed that the replacement of DIDP by ELO in the lead stabilized system appears to give rise to an undesirable increase in peak heat release rate, on the positive side the limiting oxygen index is observed to increase as well. When nanoclay is added to the lead free, ELO-stabilized systems, in contrast, an across the board improvement in fire properties is observed, with reduced

PHRR and increased LOI in nearly every case. As a result, three out of four lead-free, ELO-plasticized nanocomposite systems match or exceed the control in terms of both PHRR and LOI values.

Based on the results obtained to date, the two lead- and phthalate-free systems with performance profiles most closely matched to the lead stabilized, DIDP plasticized control are shown in Table 7.

Table 7 – Comparison of Lead Stabilized, DIDP Plasticized Control with Optimized Non-Lead Stabilized, ELO plasticized PVC Nanocomposite Formulations

Property	A (control)	L	M
T_{onset} / T_{max}, TGA in air (°C)	264 / 304	281 / 311	275 / 286
Static stability failure (minutes at 210 °C)	20	20	10
Dynamic stability failure (minutes at 210 °C, 150 rpm)	48	18	10
100% / break stress (MPa)	17 / 22	19 / 25	22 / 25
Break strain	180%	180%	150%
Hardness (Shore A)	84	81	84
Volume resistivity (Ω/cm)	1.5×10¹⁵	2.5×10¹²	9.0×10¹³
Limiting oxygen index	28.5%	29.0%	33.0%
Peak heat release rate (kW/m ²)	270	250	270

While an exact match of properties has not been achieved, these results demonstrate that the replacement of a lead stabilizer and a phthalate plasticizer by a much more acceptable additive package consisting of a non-lead stabilizer, epoxidized linseed oil and nanoclay gives rise to very respectable properties profiles and performance on par with or better than the control in the majority of the tests performed. The enhanced environmental acceptability of these alternative formulations represents an additional and very real advantage of these systems as well. It is also emphasized that no changes in processing were necessary and that the components used were commercially available. Finally, the overall cost of these formulations, while currently higher than the control, is not so high as to not preclude their utility, especially as the price of oil continues to increase and phthalates like DIDP lose their price advantage versus epoxidized linseed

oil; the non-lead stabilizers are already cost-competitive, and the cost of the nanoclay is minimized due to the very low concentration used.

In sum, this project has succeeded in demonstrating the development of practical, high performance alternative PVC formulations with enhanced acceptability versus current additive packages. Likewise, based on the results so far, the areas where degraded performance is observed as a result of nanoclay addition should not be inherent to the nanoclays themselves, and may thus be addressed through nanofiller choice and purification. While more work is needed to confirm the statistical significance of a few of the results reported here, and a additional analyses relevant to wire and cable applications would be desirable (i.e. dielectric constant, breakdown strength, weathering/aging), further properties enhancements should be achievable in systems very similar to those reported here.

Acknowledgements

The authors would like to acknowledge the financial support of the Toxics Use Reduction Institute as well as the extremely generous donation of several hundred pounds of materials and substantial expertise on the part of Teknor Apex – without these two organizations supporting us, this work would not have been possible. Likewise, the facilities and general support of the Department of Plastics Engineering were equally critical to the success of this work. In particular, we thank Prof. Steve Orroth and Prof. Steve Driscoll for valuable input on the processing side, Prof. Rudy Deanin for equally valuable input (including the suggestion that ELO should be miscible with PVC) on the formulating and testing side, and Dave Rondeau for a wide range of day to day assistance.

We also thank Rajkumar Thiruvankataswamy for his assistance in processing these materials, Benjamin Bowers for his assistance with thermogravimetric analysis, Raymond Dunn and Charlie Currie for allowing us access to resistivity testing equipment, and Candace Tsai, Mike Ellenbecker, and their colleagues at the Department of Work Environment for carrying out the complimentary nanoparticle monitoring studies reported here.

References

- ¹ For additional discussion see “Environmental, Health and Safety Issues in the Coated Wire and Cable Industry”, Technical Report No. 51, prepared by Greiner Environmental, Inc. for UML TURI (<http://www.turi.org/content/content/view/full/994/>)
- ² See <http://www.honeywell.com/sites/sm/aegis/> for product descriptions.
- ³ Image from <http://www.specialchem4polymers.com/tc/Tin-stabilizers/index.aspx?id=2821>
- ⁴ González-Ortiz, L. J.; Arellano, M.; Jasso, C. F.; Mandizábal, E.; Sánchez-Peña, M. J. “Thermal stability of plasticized poly(vinyl chloride) compounds stabilized with pre-heated mixtures of calcium and/or zinc stearates” *Polymer Degradation and Stability* **90** 154 (2005).
- ⁵ Fisch, M. H.; Bacaloglu, R. “Mechanism of poly(vinyl chloride) stabilization” *Plastics, Rubber and Composites* **28** 119 (1999).
- ⁶ Bacaloglu, R.; Stewen, U. “Study of PVC Degradation Using a Fast Computer Scanning Procedure” *Journal of Vinyl & Additive Technology* **7** 149 (2001).
- ⁷ Nielsen, E.; Larsen, P. B. (Danish EPA) “Toxicological Evaluation and Limit Values for DEHP and Phthalates, other than DEHP” *Environmental Review* **6** (1996) (<http://www.mst.dk/udgiv/Publications/1996/87-7810-638-9/pdf/87-7810-638-9.PDF>)
- ⁸ See “Public Health Statement for Di (2-ethylhexyl) phthalate (DEHP)” from the U. S. Agency for Toxic Substances and Disease Registry (<http://www.atsdr.cdc.gov/toxprofiles/phs9.html>).
- ⁹ Based on discussions with Teknor Apex personnel.
- ¹⁰ See “Biochemical Plasticizers”, Factsheet 16 from the The Institute for Local Self-Reliance (http://www.carbohydrateconomy.org/library/admin/uploadedfiles/Biochemical_Plasticizers.html) for an excellent comparison of epoxidized vegetable oils to phthalates.
- ¹¹ Okieimen, F. E.; Sogbaike, C. E. “Thermal dehydrochlorination of poly(vinyl chloride) in the presence of Jatropha seed oil” *Journal of Applied Polymer Science* **57** 513 (1995).
- ¹² Gan, L. H.; Ooi, K. S.; Goh, S. H.; Gan, L. M.; Leong, Y. C. “Epoxidized Esters of Palm Olein as Plasticizers for Poly(Vinyl Chloride)” *European Polymer Journal* **31** 719 (1995).
- ¹³ Saad, A. L. G.; Sayed, W. M.; Ahmed, M. G. M.; Hassan, A. M. “Preparation and Properties of Some Filled Poly(vinyl chloride) Compositions” *Journal of Applied Polymer Science* **73** 2657 (1999).

-
- ¹⁴ Baltacıoğlu, H.; Balköse, D. “Effect of Zinc Stearate and/or Epoxidized Soybean Oil on Gelation and Thermal Stability of PVC-DOP Plastigels” *Journal of Applied Polymer Science* **74** 2488 (1999).
- ¹⁵ Kann, Y.; Billingham, N. C. “Chemiluminescence is shedding light on degradation and stabilisation of plasticised poly(vinyl chloride)” *Polymer Degradation and Stability* **85** 957 (2004).
- ¹⁶ Joseph, R.; Madhusooghanan, K. N.; Alex, R.; Varghese, S.; George, K. E.; Kuriakose, B. “Studies on epoxidised rubber seed oil as secondary plasticiser/stabiliser for polyvinyl chloride” *Plastics, Rubbers and Composites* **33** 217 (2004).
- ¹⁷ Semsarzadeh, M. A.; Mehrabzadeh, M.; Arabshahi, S. S. “Mechanical and Thermal Properties of the Plasticized PVC-ESBO” *Iranian Polymer Journal* **14** 769 (2005).
- ¹⁸ González-Ortiz, L. J.; Arellano, M.; Jasso, C. F.; Mandizábal, E.; Sánchez-Peña, M. J. “Thermal stability of plasticized poly(vinyl chloride) compounds stabilized with pre-heated mixtures of calcium and/or zinc stearates” *Polymer Degradation and Stability* **90** 154 (2005).
- ¹⁹ Lerke, I.; Szymański, W. “Radiation yield of hydrogen chloride in gamma-irradiated poly(vinyl chloride) stabilized by epoxy compounds” *Journal of Applied Polymer Science* **21** 2067 (1977).
- ²⁰ Lerke, G.; Lerke, I.; Szymański, W. “Stabilization of gamma-irradiated poly(vinyl chloride) by epoxy compounds. I. Radiation yield of hydrogen chloride and changes of epoxy group concentration in gamma-irradiated PVC-stabilizer mixtures” *Journal of Applied Polymer Science* **28** 501 (1983).
- ²¹ Lerke, G.; Lerke, I.; Szymański, W. “Stabilization of gamma-irradiated poly(vinyl chloride) by epoxy compounds. III. Conjugated double bonds and degree of unsaturation in gamma-irradiated PVC-stabilizer mixtures” *Journal of Applied Polymer Science* **28** 519 (1983).
- ²² Shang, S.; Ling, M. T. K.; Westphal, S. P.; Woo, L. “Radiation Sterilization Compatibility of Medical Packaging Materials” *Journal of Vinyl & Additive Technology* **4** 60 (1998).
- ²³ Naimian, F. “Effect of non-toxic stabilizers on the gamma stabilization of poly(vinyl chloride) at sterilizing doses” *Nuclear Instruments and Methods in Physics Research B* **151** 467 (1999).
- ²⁴ Hutzler, B. W.; Machado, L. D. B.; Lugão, A. B.; Villavicencio, A-L. C. H. “Properties of irradiated PVC plasticized with non-endocrine disruptor” *Radiation Physics and Chemistry* **57** 381 (2000).

-
- ²⁵ Khang, G.; Kong, C-S.; Rhee, J. M.; Lee, H. B. “Stabilization of nontoxic PVC formulation for gamma irradiation sterilization, I. Effect of additives” *Bio-Medical Materials and Engineering* **12** 135 (2002).
- ²⁶ Kong, C-S.; Yoon, G. H.; Khang, G.; Rhee, J. M.; Lee, H. B. “Stabilization of nontoxic PVC formulation for gamma irradiation sterilization, II. Effect of antioxidants” *Bio-Medical Materials and Engineering* **12** 211 (2002).
- ²⁷ Fisch, M. H.; Bacaloglu, R. “Mechanism of poly(vinyl chloride) stabilization” *Plastics, Rubber and Composites* **28** 119 (1999).
- ²⁸ Image from “What's happening during PVC degradation?” from the Arkema-sponsored Tin Stabilizers Center (<http://www.specialchem4polymers.com/tc/Tin-Stabilizers/index.aspx?id=2821>)
- ²⁹ Kovačić, T.; Mrklić, Z. “The kinetic parameters for the evaporation of plasticizers from plasticized poly(vinyl chloride)” *Thirmichimica Acta* **381** 49 (2002).
- ³⁰ Gibbons, W. S.; Kusy, R. P. “Effects of plasticization on the dielectric properties of poly(vinyl chloride) membranes” *Thirmochimica Acta* **284** 21 (1996).
- ³¹ Harris, E.; Braun, D. (Union Carbide Corp.) “Wire and cable insulation comprising vinyl chloride polymer and lacton graft copolymer” *U. S. Patent 3,855,357* (1974).
- ³² Brecker, L. R.; Keeley, C.; Brilliant, S. D. (Argus Chemical) “Polyvinyl chloride resin compositions having a high volume resistivity and resistance to deterioration when heated at temperatures above 100 degrees C” *U. S. Patent 4,447,569* (1984).
- ³³ Chu-Ba, C. (Capital Wire & Cable Corp.) “Insulated electrical products and processes of forming such products” *U. S. Patent 4,806,425* (1989).
- ³⁴ Kroushl III, P. W. (Cooper Industries, Inc.) “Polyvinyl chloride based plenum cable” *U. S. Patent 5,227,417* (1993).
- ³⁵ Saad, A. L. G.; Sayed, W. M.; Ahmed, M. G. M.; Hassan, A. M. “Preparation and Properties of Some Filled Poly(vinyl chloride) Compositions” *Journal of Applied Polymer Science* **73** 2657 (1999).
- ³⁶ J-C. Huang; R. D. Deanin “Concentration Dependency of Interaction Parameter Between PVC and Plasticizers Using Inverse Gas Chromatography” *Journal of Applied Polymer Science* **91** 146 (2004).
- ³⁷ Based on discussions with Prof. R. Deanin, UML Plastics Engineering.
- ³⁸ Adeka ADK CIZER O-series
(<http://www.adk.co.jp/en/chemical/products/pvc/index.html>)
- ³⁹ Akzo-Nobel Lankroflex L
(<http://www.akros.com/PVC+Products/Product+Information-Europe/Epoxy/>)

-
- ⁴⁰ Arkema Vikoflex 7190 (<http://www.arkema-inc.com/index.cfm?pag=16>)
- ⁴¹ C. P. Hall PLASTHALL ELO
(http://www.cphall.com/partner_integration/productcleanup.nsf/vAll_ID/487653AB62AF12EE86256F9D0071661B?OpenDocument)
- ⁴² Cognis EDENOL B 316 SPEZIAL
(http://www.cognis.com/agrosolutions/pdfs/Global_Product_Line.pdf#search=%22edeno1%20B%20316%22)
- ⁴³ Crompton Drapex 10.4
(http://www.cromptoncorp.com/servlet/ContentServer?pagename=Crompton/ck_prod/product&c=ck_prod&cid=990576523951&countryid=990049203009&invoker=results&p=985964216258)
- ⁴⁴ Dow FLEXOL (http://www.dow.com/products_services/prodinfo.htm)
- ⁴⁵ Gibbons, W. S.; Patel, H. M.; Kusy, R. P. “Effects of plasticizers on the mechanical properties of poly(vinyl chloride) membranes for electrodes and biosensors” *Polymer* **38** 2633 (1997).
- ⁴⁶ Messersmith, P. B.; Giannelis, E. P. “Synthesis and Characterization of Layered Silicate-Epoxy Nanocomposites” *Chemistry of Materials* **6** 1719 (1994).
- ⁴⁷ Brown, J. M.; Curliss, D.; Vaia, R. A. “Thermoset-Layered Silicate Nanocomposites. Quaternary Ammonium Montmorillonite with Primary Diamine Cured Epoxies” *Chemistry of Materials* **12** 3376 (2000).
- ⁴⁸ Chen, J-S.; Poliks, M. D.; Ober, C. K.; Zhang, Y.; Wiesner, U.; Giannelis, E. “Study of the interlayer expansion mechanism and thermal–mechanical properties of surface-initiated epoxy nanocomposites” *Polymer* **43** 4895 (2002).
- ⁴⁹ Ishida, H.; Campbell, S.; Blackwell, J. “General Approach to Nanocomposite Preparation” *Chemistry of Materials* **12** 1260 (2000).
- ⁵⁰ Wan, C.; Qiao, X.; Zhang, Y.; Zhang, Y. “Effect of Epoxy Resin on Morphology and Physical Properties of PVC/Organophilic Montmorillonite Nanocomposites” *Journal of Applied Polymer Science* **89** 2184 (2003).
- ⁵¹ Miyagawa, H.; Mohanty, A.; Drzal, L. T.; Misra, M. “Effect of Clay and Alumina-Nanowhisker Reinforcements on the Mechanical Properties of Nanocomposites from Biobased Epoxy: A Comparative Study” *Industrial & Engineering Chemistry Research* **43** 7001 (2004).

-
- ⁵² Miyagawa, H.; Misra, M.; Drzal, L. T.; Mohanty, A. K. "Novel biobased nanocomposites from functionalized vegetable oil and organically-modified layered silicate clay" *Polymer* **46** 445 (2005).
- ⁵³ Miyagawa, H.; Misra, M.; Drzal, L. T.; Mohanty, A. K. "Biobased Epoxy/Layered Silicate Nanocomposites: Thermophysical Properties and Fracture Behavior Evaluation" *Journal of Polymers and the Environment* **13** 87 (2005).
- ⁵⁴ LeBaron, P. C.; Wang, Z.; Pinnavaia, T. J. "Polymer-layered silicate nanocomposites: an overview" *Applied Clay Science* **15** 11 (1999).
- ⁵⁵ Alexandre, M.; DuBois, P. "Polymer-layered silicate nanocomposites: preparation, properties and uses of a new class of materials" *Materials Science and Engineering R: Reports* **28** 1 (2000).
- ⁵⁶ Schmidt, D. F.; Shah, D.; Giannelis, E. P. "New advances in polymer/layered silicate nanocomposites" *Current Opinions in Solid State and Materials Science* **6** 205 (2002).
- ⁵⁷ Wang, D.; Parlow, D.; Yao, Q.; Wilkie C. "PVC-Clay Nanocomposites: Preparation, Thermal and Mechanical Properties" *Journal of Vinyl & Additive Technology* **7** 203 (2001).
- ⁵⁸ Du, J.; Wang, D.; Wilkie, C.; Wang, J. "An XPS investigation of thermal degradation and charring on poly(vinyl chloride)-clay nanocomposites" *Polymer Degradation and Stability* **79** 319 (2003).
- ⁵⁹ Kim, Y.; White, J. L. "Melt-Intercalation Nanocomposites with Chlorinated Polymers" *Journal of Applied Polymer Science* **90** 1581 (2003).
- ⁶⁰ Yalcin, B.; Cakmak, M. "The role of plasticizer on the exfoliation and dispersion and fracture behavior of clay particles in PVC matrix: a comprehensive morphological study" *Polymer* **45** 6623 (2004).
- ⁶¹ Yoo, Y.; Kim, S-S.; Won, J. C.; Choi, K-Y.; Lee, J. H. "Enhancement of the thermal stability, mechanical properties and morphologies of recycled PVC/clay nanocomposites" *Polymer Bulletin* **52** 373 (2004).
- ⁶² Kovarova, L.; Kalendova, A.; Simonik, J.; Malac, J.; Weiss, Z.; Gerard, J. F. "Effect of melt processing conditions on mechanical properties of polyvinylchloride/organoclay nanocomposites" *Plastics, Rubbers and Composites* **33** 287 (2004).
- ⁶³ Kovarova, L.; Kalendova, A.; Gerard, J. F.; Malac, J.; Simonik, J.; Weiss, Z. "Structure Analysis of PVC Nanocomposites" *Macromolecular Symposia* **221** 105 (2005).
- ⁶⁴ Yalcin, B.; Cakmak, M. "Molecular Orientation Behavior of Poly(vinyl chloride) as Influenced by the Nanoparticles and Plasticizer during Uniaxial Film Stretching in the Rubbery Stage" *Journal of Polymer Science B* **43** 724 (2005).

⁶⁵ See “Key Properties of Montmorillonite”, from Southern Clay Products (<http://nanoclay.com/keyproperties.asp>).

⁶⁶ See “Cloisite 30B Typical Physical Properties Bulletin”, from Southern Clay Products (http://www.scpod.com/product_bulletins/PB%20Cloisite%2030B.pdf)

⁶⁷ Swindells, J. & Murray, M., eds. “Electrical Wire Handbook, Part 1 – Wire and Cable Production Material” Wire Association International: Guilford, 2003; p. 87

Appendix A indicates the compositions of the different PVC compounds referred to by italicized letters in the text.

Table A- 1:- Notation of symbols used to denote the samples

S.No	Sample	Stabilizer	Plasticizer	OMMT
1	<i>A</i>	Pb	DIDP	N/A
2	<i>B</i>	Ca/Mg/Zn	DIDP	N/A
3	<i>C</i>	Ca/Zn	DIDP	N/A
4	<i>D</i>	Mixed metal, lubricating	DIDP	N/A
5	<i>E</i>	Ca/Zn, lubricating	DIDP	N/A
6	<i>F</i>	Pb	ELO	N/A
7	<i>G</i>	Ca/Mg/Zn	DIDP	2%
8	<i>H</i>	Ca/Zn	DIDP	2%
9	<i>I</i>	Mixed metal, lubricating	DIDP	2%
10	<i>J</i>	Ca/Zn, lubricating	DIDP	2%
11	<i>K</i>	Ca/Mg/Zn	ELO	2%
12	<i>L</i>	Ca/Zn	ELO	2%
13	<i>M</i>	Mixed metal, lubricating	ELO	2%
14	<i>N</i>	Ca/Zn, lubricating	ELO	2%
15	<i>O</i>	Ca/Mg/Zn	ELO	N/A
16	<i>P</i>	Ca/Zn	ELO	N/A
17	<i>Q</i>	Mixed metal, lubricating	ELO	N/A
18	<i>R</i>	Ca/Zn, lubricating	ELO	N/A

Note:

- Pb - Halstab 60 lead sulfate tribasic / lead phthalate dibasic stabilizer
- Ca/Mg/Zn – Non-Pb 1 stabilizer
- Ca/Zn – Non-Pb 2 stabilizer
- Mixed metal, lubricating – Non-Pb 3 stabilizer
- Ca/Zn, lubricating – Non-Pb 4 stabilizer
- DIDP – Diisodecyl phthalate (see Figure 3 for structure)
- ELO – Arkema Vikoflex 7190 epoxidized linseed oil (see Figure 3 for structure)
- OMMT – Southern Clay Cloisite 30B (see Figure 2 for modifier structure)
- N/A – Not applicable

APPENDIX B**Formulations**

Appendix B gives the full composition of each formulation used in this study.

Table B-1 Shows the Control Sample A Formulation (commercial PVC formulation – Pb + DIDP)

Raw Material	Description	p/hr	Wt %	Weight in grams
PVC -2100	PVC resin (K ~ 67)	100	50.83	1524.9
DIDP N	Plasticizer	55	27.95	838.5
Atomite (CaCO ₃)	Filler	12	6.1	183
SP - 33 (Kaolin clay)	Filler	22	11.18	335.4
R flake	Lubricant	0.25	0.13	3.9
Antimony trioxide	Fire retardant	2.5	1.27	38.1
Halstab 60	Lead Stabilizer	5	2.54	76.2
Total		196.75	100	3000

Table B-2 Shows the Sample B Formulation (Non Pb 1 + DIDP)

Raw Material	Description	p/hr	Wt %	Weight in grams
PVC -2100	PVC resin (K ~ 67)	100	50.83	1524.9
DIDP N	Plasticizer	55	27.95	838.5
Atomite (CaCO ₃)	Filler	12	6.1	183
SP - 33 (Kaolin clay)	Filler	22	11.18	335.4
R flake	Lubricant	0.25	0.13	3.9
Antimony trioxide	Fire retardant	2.5	1.27	38.1
Non-Pb 1	Ca/Mg/Zn stabilizer	5	2.54	76.2
Total		196.75	100	3000

Table B-3 Shows the Sample C Formulation (Non Pb 2 + DIDP)

Raw Material	Description	p/hr	Wt %	Weight in grams
PVC -2100	PVC resin (K ~ 67)	100	50.83	1524.9
DIDP N	Plasticizer	55	27.95	838.5
Atomite (CaCO ₃)	Filler	12	6.1	183
SP - 33 (Kaolin clay)	Filler	22	11.18	335.4
R flake	Lubricant	0.25	0.13	3.9
Antimony trioxide	Fire retardant	2.5	1.27	38.1
Non-Pb 2	Ca/Zn stabilizer	5	2.54	76.2
Total		196.75	100	3000

APPENDIX B**Formulations****Table B-4 Shows the Sample D Formulation (Non Pb 3 + DIDP)**

Raw Material	Description	p/hr	Wt %	Weight in grams
PVC -2100	PVC resin (K ~ 67)	100	50.8906	1526.72
DIDP N	Plasticizer	55	27.9898	839.695
Atomite (CaCO ₃)	Filler	12	6.10687	183.206
SP - 33 (Kaolin clay)	Filler	22	11.1959	335.878
Antimony trioxide	Fire retardant	2.5	1.27226	38.1679
Non-Pb 3	Mixed metal lubricating stabilizer	5	2.54453	76.3359
Total		196.5	100	3000

Table B-5 Shows the Sample E Formulation (Non Pb 4 + DIDP)

Raw Material	Description	p/hr	Wt %	Weight in grams
PVC -2100	PVC resin (K ~ 67)	100	50.8906	1526.72
DIDP N	Plasticizer	55	27.9898	839.695
Atomite (CaCO ₃)	Filler	12	6.10687	183.206
SP - 33 (Kaolin clay)	Filler	22	11.1959	335.878
Antimony trioxide	Fire retardant	2.5	1.27226	38.1679
Non-Pb 4	Ca / Zn lubricating stabilizer	5	2.54453	76.3359
Total		196.5	100	3000

Table B-6 Shows the Sample F Formulation (Pb + ELO)

Raw Material	Description	p/hr	Wt %	Weight in grams
PVC -2100	PVC resin (K ~ 67)	100	50.83	1524.9
ELO	Plasticizer	55	27.95	838.5
Atomite (CaCO ₃)	Filler	12	6.1	183
SP - 33 (Kaolin clay)	Filler	22	11.18	335.4
R flake	Lubricant	0.25	0.13	3.9
Antimony trioxide	Fire retardant	2.5	1.27	38.1
Halstab 60	Lead Stabilizer	5	2.54	76.2
Total		196.75	100	3000

APPENDIX B**Formulations****Table B-7 Shows the Sample G Formulation (Non Pb 1 + DIDP + 2% NC)**

Raw Material	Description	phr	Wt %	Weight in grams
PVC -2100	PVC resin (K ~ 67)	100	49.82	1494.6
DIDP N	Plasticizer	55	27.40	822
Atomite (CaCO ₃)	Filler	12	5.98	179.4
SP - 33 (Kaolin clay)	Filler	22	10.96	328.8
R flake	Lubricant	0.25	0.124	3.72
Antimony trioxide	Fire retardant	2.5	1.25	37.5
Non-Pb 1	Ca/Mg/Zn stabilizer	5	2.5	75
Cloisite 30 B	Nanoclay	4	2	60
Total		200.75	~100	~3000

Table B-8 Shows the Sample H Formulation (Non Pb 2 + DIDP + 2% NC)

Raw Material	Description	phr	Wt %	Weight in grams
PVC -2100	PVC resin (K ~ 67)	100	49.82	1494.6
DIDP N	Plasticizer	55	27.40	822
Atomite (CaCO ₃)	Filler	12	5.98	179.4
SP - 33 (Kaolin clay)	Filler	22	10.96	328.8
R flake	Lubricant	0.25	0.124	3.72
Antimony trioxide	Fire retardant	2.5	1.25	37.5
Non-Pb 2	Ca/Zn stabilizer	5	2.5	75
Cloisite 30 B	Nanoclay	4	2	60
Total		200.75	~100	~3000

Table B-9 Shows the Sample I Formulation (Non Pb 3 + DIDP + 2% NC)

Raw Material	Description	phr	Wt %	Weight in grams
PVC -2100	PVC resin (K ~ 67)	100	49.88	1496.4
DIDP N	Plasticizer	55	27.43	822.9
Atomite (CaCO ₃)	Filler	12	5.99	179.7
SP - 33 (Kaolin clay)	Filler	22	10.97	329.1
Antimony trioxide	Fire retardant	2.5	1.25	37.5
Non-Pb 3	Mixed metal lubricating stabilizer	5	2.5	75
Cloisite 30 B	Nanoclay	4	2	60
Total		200.5	~100	~3000

APPENDIX B

Formulations

Table B-10 Shows the Sample J Formulation (Non Pb 4 + DIDP + 2% NC)

Raw Material	Description	p/hr	Wt %	Weight in grams
PVC -2100	PVC resin (K ~ 67)	100	49.88	1496.4
DIDP N	Plasticizer	55	27.43	822.9
Atomite (CaCO ₃)	Filler	12	5.99	179.7
SP - 33 (Kaolin clay)	Filler	22	10.97	329.1
Antimony trioxide	Fire retardant	2.5	1.25	37.5
Non-Pb 4	Ca / Zn lubricating stabilizer	5	2.5	75
Cloisite 30 B	Nanoclay	4	2	60
Total		200.5	~100	~3000

Table B-11 Shows the Sample K Formulation (Non Pb 1 + ELO + 2% NC)

Raw Material	Description	p/hr	Wt %	Weight in grams
PVC -2100	PVC resin (K ~ 67)	100	49.82	1494.6
ELO	Plasticizer	55	27.40	822
Atomite (CaCO ₃)	Filler	12	5.98	179.4
SP - 33 (Kaolin clay)	Filler	22	10.96	328.8
R flake	Lubricant	0.25	0.124	3.72
Antimony trioxide	Fire retardant	2.5	1.25	37.5
Non-Pb 1	Ca/Mg/Zn stabilizer	5	2.5	75
Cloisite 30 B	Nanoclay	4	2	60
Total		200.75	~100	~3000

Table B-12 Shows the Sample L Formulation (Non Pb 2 + ELO + 2% NC)

Raw Material	Description	p/hr	Wt %	Weight in grams
PVC -2100	PVC resin (K ~ 67)	100	49.82	1494.6
ELO	Plasticizer	55	27.40	822
Atomite (CaCO ₃)	Filler	12	5.98	179.4
SP - 33 (Kaolin clay)	Filler	22	10.96	328.8
R flake	Lubricant	0.25	0.124	3.72
Antimony trioxide	Fire retardant	2.5	1.25	37.5
Non-Pb 2	Ca/Zn stabilizer	5	2.5	75
Cloisite 30 B	Nanoclay	4	2	60
Total		200.75	~100	~3000

APPENDIX B

Formulations

Table B-13 Shows the Sample M Formulation (Non Pb 3 + ELO + 2% NC)

Raw Material	Description	p/hr	Wt %	Weight in grams
PVC -2100	PVC resin (K ~ 67)	100	49.88	1496.4
ELO	Plasticizer	55	27.43	822.9
Atomite (CaCO ₃)	Filler	12	5.99	179.7
SP - 33 (Kaolin clay)	Filler	22	10.97	329.1
Antimony trioxide	Fire retardant	2.5	1.25	37.5
Non-Pb 3	Mixed metal lubricating stabilizer	5	2.5	75
Cloisite 30 B	Nanoclay	4	2	60
Total		200.5	~100	~3000

Table B-14 Shows the Sample N Formulation (Non Pb 4 + ELO+ 2% NC)

Raw Material	Description	p/hr	Wt %	Weight in grams
PVC -2100	PVC resin (K ~ 67)	100	49.88	1496.4
ELO	Plasticizer	55	27.43	822.9
Atomite (CaCO ₃)	Filler	12	5.99	179.7
SP - 33 (Kaolin clay)	Filler	22	10.97	329.1
Antimony trioxide	Fire retardant	2.5	1.25	37.5
Non-Pb 4	Ca / Zn lubricating stabilizer	5	2.5	75
Cloisite 30 B	Nanoclay	4	2	60
Total		200.5	~100	~3000

Table B-15 Shows the Sample O Formulation (Non Pb 1 + ELO)

Raw Material	Description	p/hr	Wt %	Weight in grams
PVC -2100	PVC resin (K ~ 67)	100	50.83	1524.9
ELO	Plasticizer	55	27.95	838.5
Atomite (CaCO ₃)	Filler	12	6.1	183
SP - 33 (Kaolin clay)	Filler	22	11.18	335.4
R flake	Lubricant	0.25	0.13	3.9
Antimony trioxide	Fire retardant	2.5	1.27	38.1
Non-Pb 1	Ca/Mg/Zn stabilizer	5	2.54	76.2
Total		196.75	100	3000

APPENDIX B

Formulations

Table B-16 Shows the Sample P Formulation (Non Pb 2 + ELO)

Raw Material	Description	phr	Wt %	Weight in grams
PVC -2100	PVC resin (K ~ 67)	100	50.83	1524.9
ELO	Plasticizer	55	27.95	838.5
Atomite (CaCO ₃)	Filler	12	6.1	183
SP - 33 (Kaolin clay)	Filler	22	11.18	335.4
R flake	Lubricant	0.25	0.13	3.9
Antimony trioxide	Fire retardant	2.5	1.27	38.1
Non-Pb 2	Ca/Zn stabilizer	5	2.54	76.2
Total		196.75	100	3000

Table B-17 Shows the Sample Q Formulation (Non Pb 3 + ELO)

Raw Material	Description	phr	Wt %	Weight in grams
PVC -2100	PVC resin (K ~ 67)	100	50.8906	1526.72
ELO	Plasticizer	55	27.9898	839.695
Atomite (CaCO ₃)	Filler	12	6.10687	183.206
SP - 33 (Kaolin clay)	Filler	22	11.1959	335.878
Antimony trioxide	Fire retardant	2.5	1.27226	38.1679
Non-Pb 3	Mixed metal lubricating stabilizer	5	2.54453	76.3359
Total		196.5	100	3000

Table B-18 Shows the Sample R Formulation (Non Pb 4 + ELO)

Raw Material	Description	phr	Wt %	Weight in grams
PVC -2100	PVC resin (K ~ 67)	100	50.8906	1526.72
ELO	Plasticizer	55	27.9898	839.695
Atomite (CaCO ₃)	Filler	12	6.10687	183.206
SP - 33 (Kaolin clay)	Filler	22	11.1959	335.878
Antimony trioxide	Fire retardant	2.5	1.27226	38.1679
Non-Pb 4	Ca / Zn lubricating stabilizer	5	2.54453	76.3359
Total		196.5	100	3000

Appendix C indicates the screw programming used in the twin screw extruder during melt blending of the PVC and PVC nanocomposites compounds.

Table C-1 Shows the Low Shear PVC Screw Programming

Element type	Number of Elements
O Ring	1
14 * 14	1
42 * 42	4
28 * 28	5
20 * 20	4
28 * 28	1
14 * 14	11
KB 45 * 5 * 20	2
KB 45 * 5 * 14 (LH)	1
14 * 14	1
28 * 28	1
42 * 42	2
20 * 20	3
14* 14	4
Screw tip	1

Appendix D gives the processing parameters found to be most effective during the twin screw extrusion of the dry blend and the sheet extrusion of the melt compounded pellets.

Table D-1 Shows the Twin Screw Extrusion Processing Parameters

S.No	Sample	Feed rate	Screw speed, rpm	Torque, %	Melt Temp., °C	Pressure, psi	Pelletizer speed
1	A	5.2	63	30	165	N/A	2.5
2	B	5.2	62	30	164	N/A	2.5
3	C	5.2	62	31	165	N/A	2.5
4	D	5.2	72	28	166	N/A	2.5
5	E	5.5	77	27	166	N/A	2.5
6	F	5.5	75	27	164	N/A	2.5
7	G	4	80	26	166	N/A	2.5
8	H	4.3	80	27	167	N/A	2.6
9	I	4.3	80	28	168	N/A	2.6
10	J	4.3	80	30	166	N/A	2.6
11	K	4.0	80	30	167	N/A	2.6
12	L	5	46	30	164	570	2.5
13	M	5.5	80	25	165	530	2.5
14	N	5.5	86	29	167	560	2.0
15	O	5.5	86	27	166	540	2.0
16	P	6.5	80	27	166	510	2.0
17	Q	6.0	84	26	168	520	2.0
18	R	6.0	84	27	166	535	2.0

Table D-2 Shows the Sheet Extrusion Processing Parameters

S.No	Sample	Screw speed, rpm	Torque, %	Melt Temp., °F / °C	Pressure, psi		Stack speed, rpm	Thickness, mm
					Before breaker plate	After breaker plate		
1	A	34	37	350 / 177	950	700	2.4	0.78
2	B	34	37	349 / 176	990	710	2.4	0.70
3	C	34	36	349 / 176	1020	720	2.4	0.98
4	D	34	39	350 / 177	1080	750	3.1	0.82
5	E	34	40	349 / 176	1140	810	2.8	0.81
6	F	34	44	349 / 176	1240	930	2.5	0.75
7	G	15	21	350 / 177	1250	710	2.4	0.95
8	H	15	22	349 / 176	1270	730	2.4	0.75
9	I	13	23	350 / 177	1540	640	2.1	0.83
10	J	13	20	346 / 174	1480	660	2.1	0.75
11	K	13	43	348 / 176	2100	980	1.9	0.87
12	L	17	19	356 / 180	3950	900	2.4	0.80
13	M	17	24	343 / 173	4080	960	2.4	0.89
14	N	17	37	343 / 173	3980	840	2.4	0.90
15	O	17	37	356 / 180	3990	860	2.4	0.82
16	P	17	28	356 / 180	2400	620	2.4	0.82
17	Q	17	34	356 / 180	3540	810	2.4	0.80
18	R	17	35	356 / 180	3460	830	2.4	0.85

APPENDIX E**Nanoparticle Analysis****Table E -1 Shows the activities and measurement location observed during the weighing process**

Time	Activity	Measurement Location
10:51 AM – 10:55 AM	No activity	Measure background four feet from mixer
10:56 AM – 10:57 AM	Nanoclay weighing process	Near operator hands
10:57 AM – 11:03 AM	Nanoclay weighing process	Operator breathing zone
11:03 AM	Kaolin clay weighing process	One foot from source
11:04 AM – 11:06 AM	Kaolin clay weighing process	Operator breathing zone
11:07 AM – 11:08 AM	Calcium carbonate weighing process	One foot from source
11:09 AM – 11:10 AM	Calcium carbonate weighing process	Operator breathing zone

Table E -2 Shows the activities and measurement location observed during the dry blending process

Time	Activity	Measurement Location
11:11 AM – 11:14 AM	No activity	Measure background four feet from mixer
11:15 AM – 11:16 AM	Add PVC and heat stabilizer to the mixer	One foot from source
11:17 AM – 11:55 AM	Mixing process	Four feet from mixer
11:56 AM -11:59 AM	Add ELO plasticizer	Four feet from mixer
12:00 PM – 12:04 PM	Add three fillers (CaCO ₃ , Kaolin clay, and nanoclay)	1 foot from mixer
12:05 PM – 12:06 PM	Mixing process	Four feet from mixer
12:07 PM	Add lubricant	Operator breathing zone
12:08 PM – 12:11 PM	Mixing process	Four feet from mixer
12:12 PM – 12:20 PM	Cooling process	Four feet from mixer
12:21 PM – 12:23 PM	Take mixture out of the mixer	1 foot from mixer
12:24 PM	Manually clean out mixer	1 foot from mixer
12:25 PM – 12:26 PM	Vacuum clean the mixer	Operator breathing zone
12:27 PM	Turn off FMPS	

Table E -3 Shows the activities and measurement location observed during the twin screw extrusion process

Time	Activity	Measurement Location
2:01 PM – 2:04 PM	No activity	Measure background four feet from extruder
2:05 PM – 2:07 PM	Pour mixture into feeder	1 foot from top of feeder
2:08 PM	Mixture entering the extruder	1 foot from bottom of feeder
2:09 PM – 2:10 PM	Extrusion	1 foot from end of extruder
2:11 PM – 2:13 PM	Extrusion	1 foot from opening in the extruder
2:14 PM – 2:47 PM	Adjust extrusion settings	Measure background four feet from extruder
2:48 PM – 2:56 PM	Extrusion	1 foot from bottom of feeder
2:57 PM – 3:04 PM	Extrusion	1 foot from end of extruder
3:05 PM	Turn off FMPS	

Figure F – 1 Shows the main effects plot for degradation onset temperature

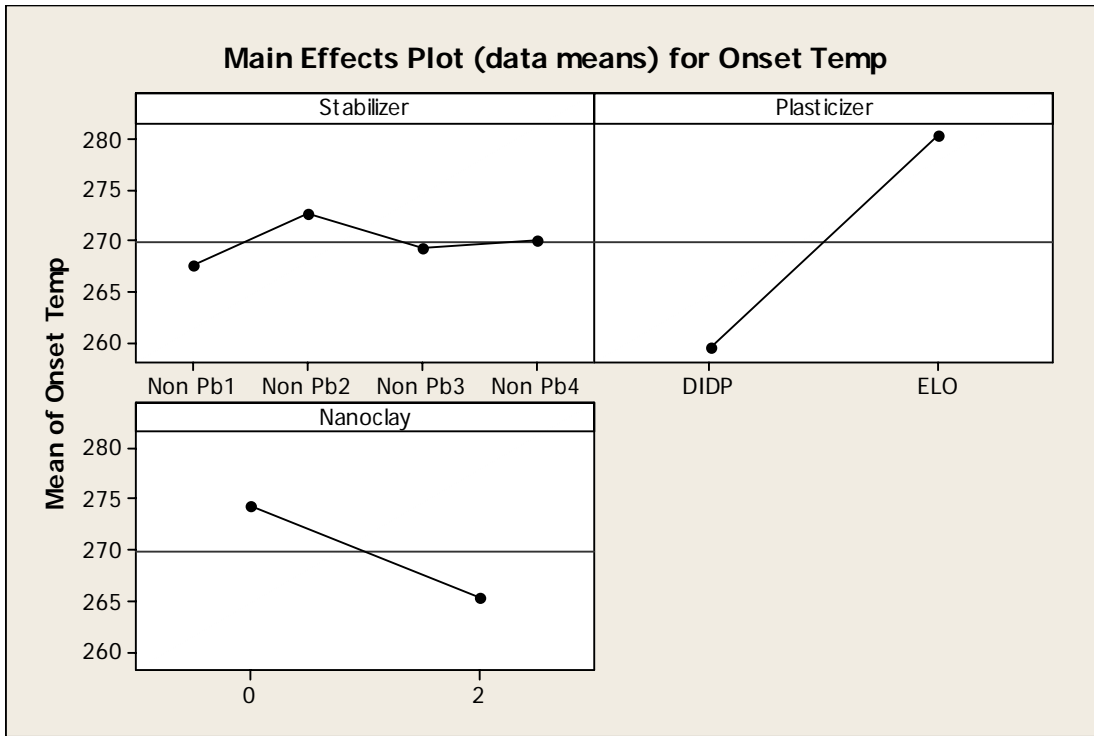


Figure F – 2 Shows the interaction effects plot for degradation onset temperature

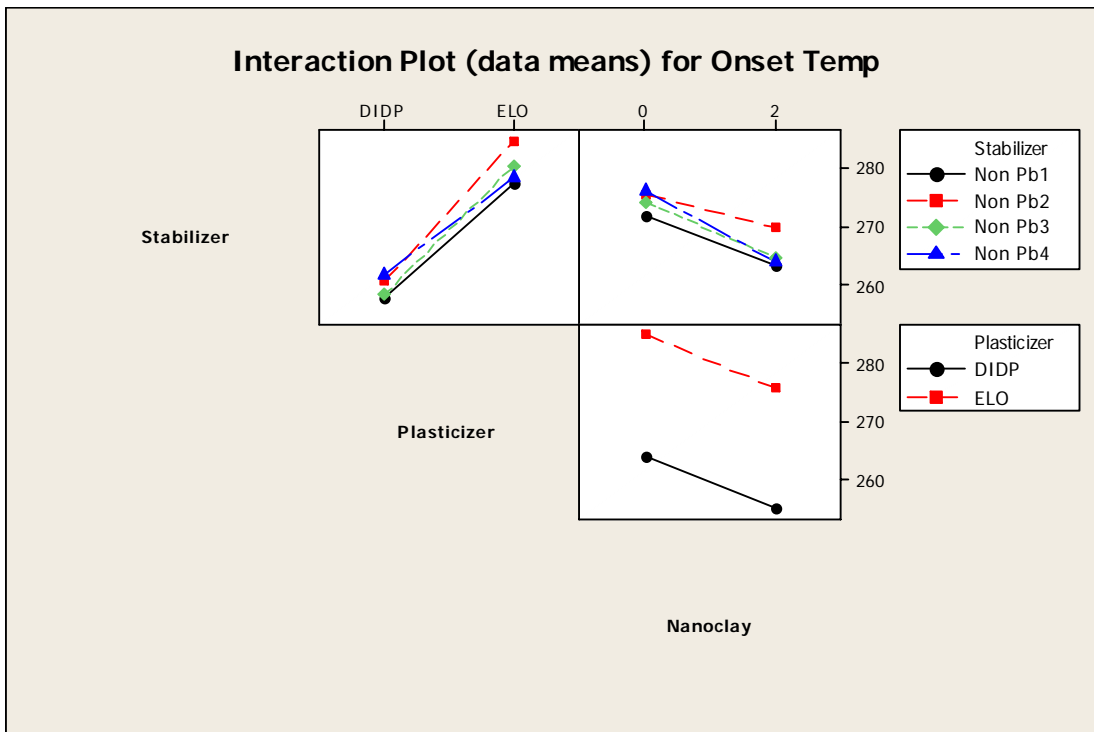


Figure F – 3 Shows the main effects plot for temperature of maximum degradation

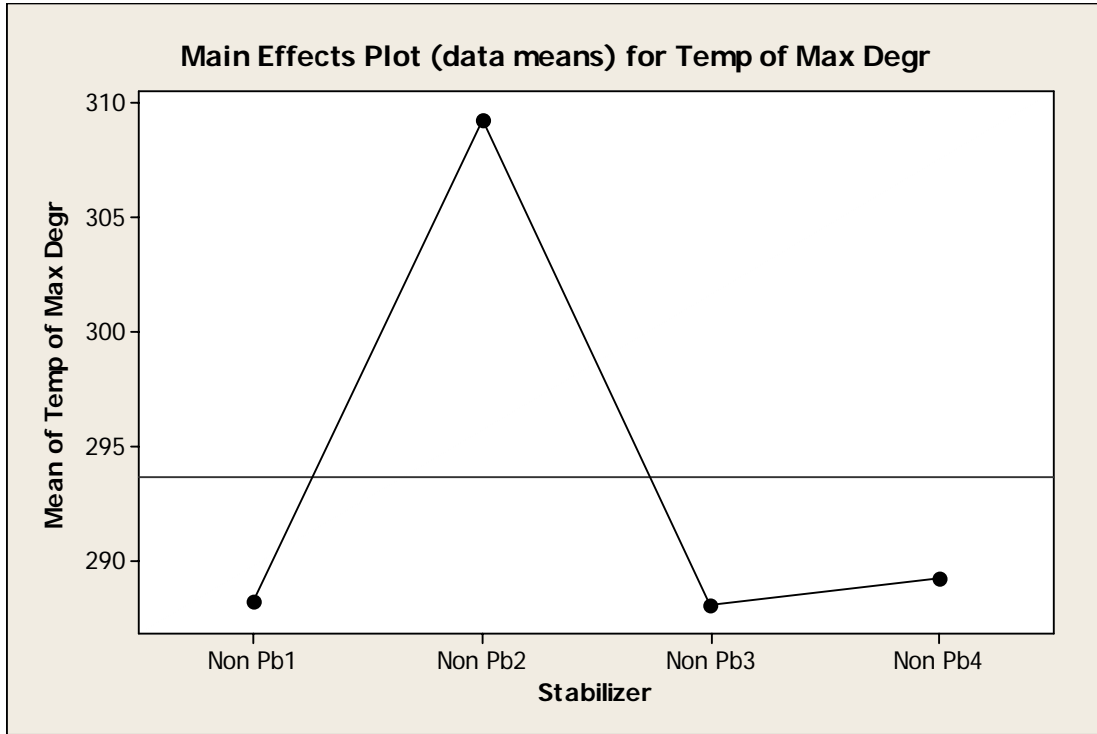


Figure G – 1 Shows the main effects plot for tensile strength at break

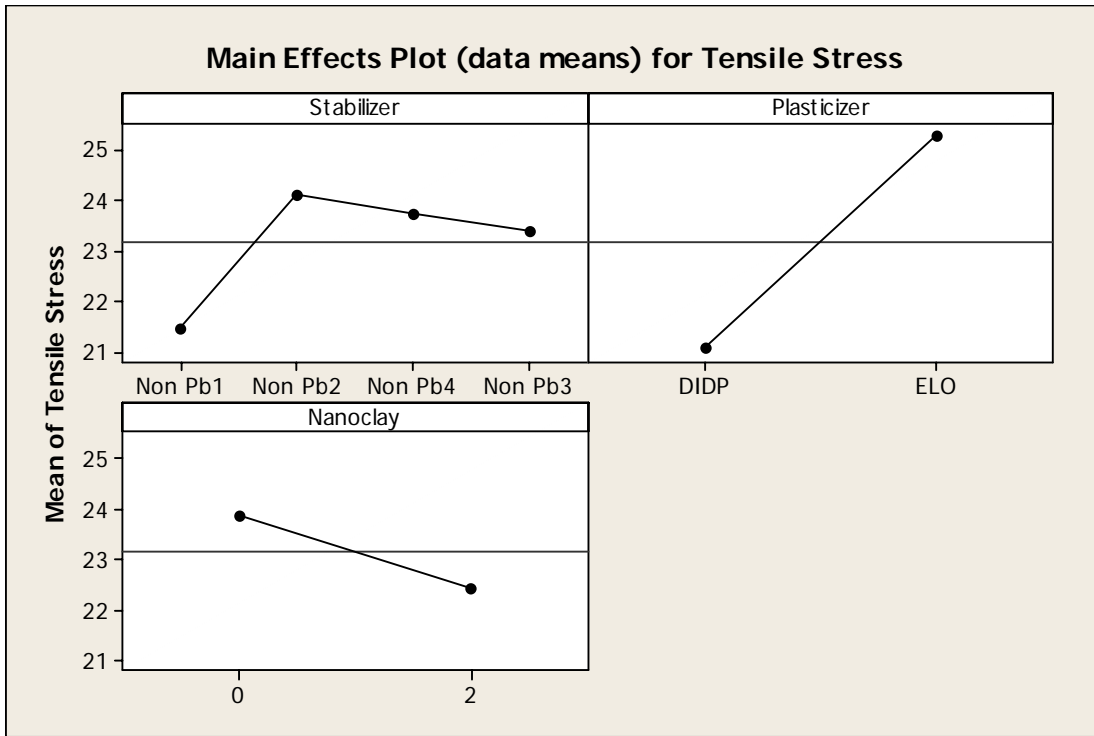


Figure G – 2 Shows the interaction effects plot for tensile strength at break

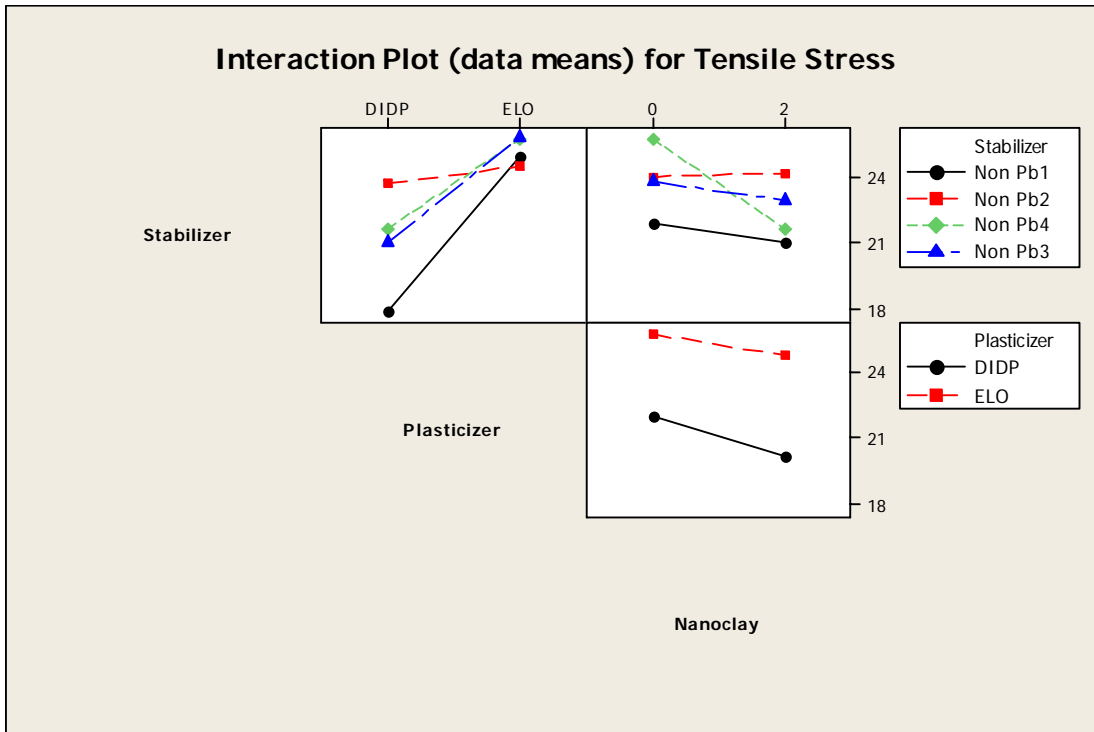


Figure G – 3 Shows the main effects plot for tensile strain at break

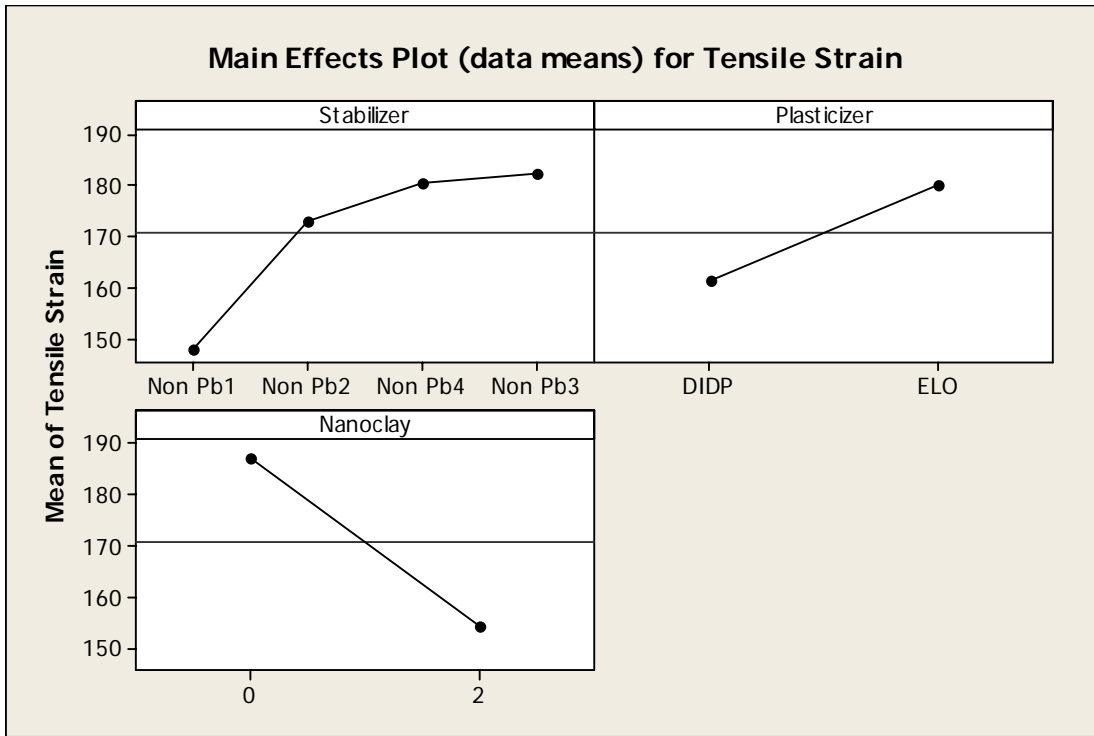


Figure G – 4 Shows the interaction effects plot for tensile strength at break

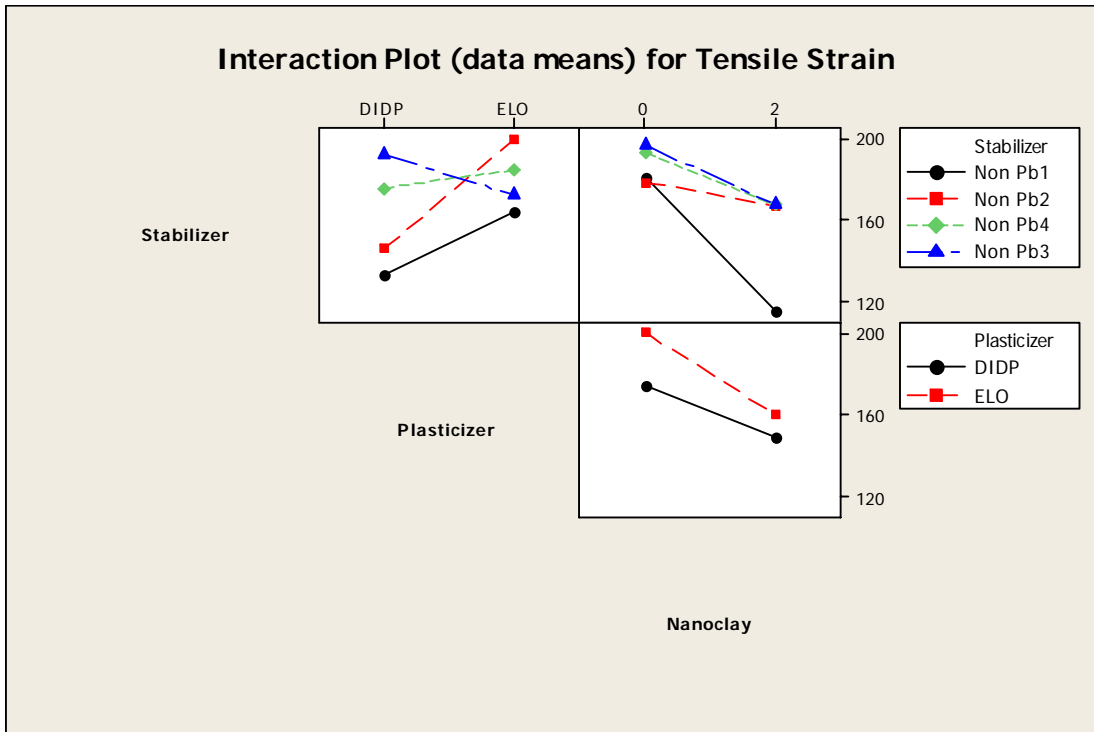


Figure G – 5 Shows the main effects plot for secant modulus

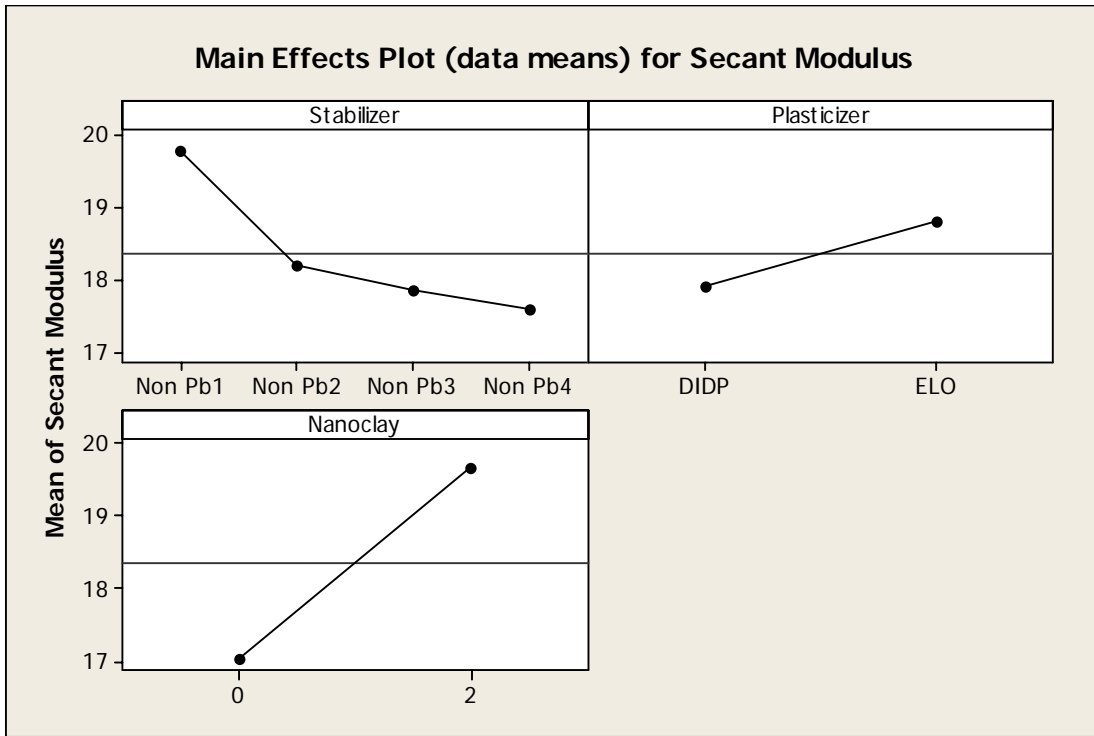


Figure G – 6 Shows the interaction effects plot for secant modulus

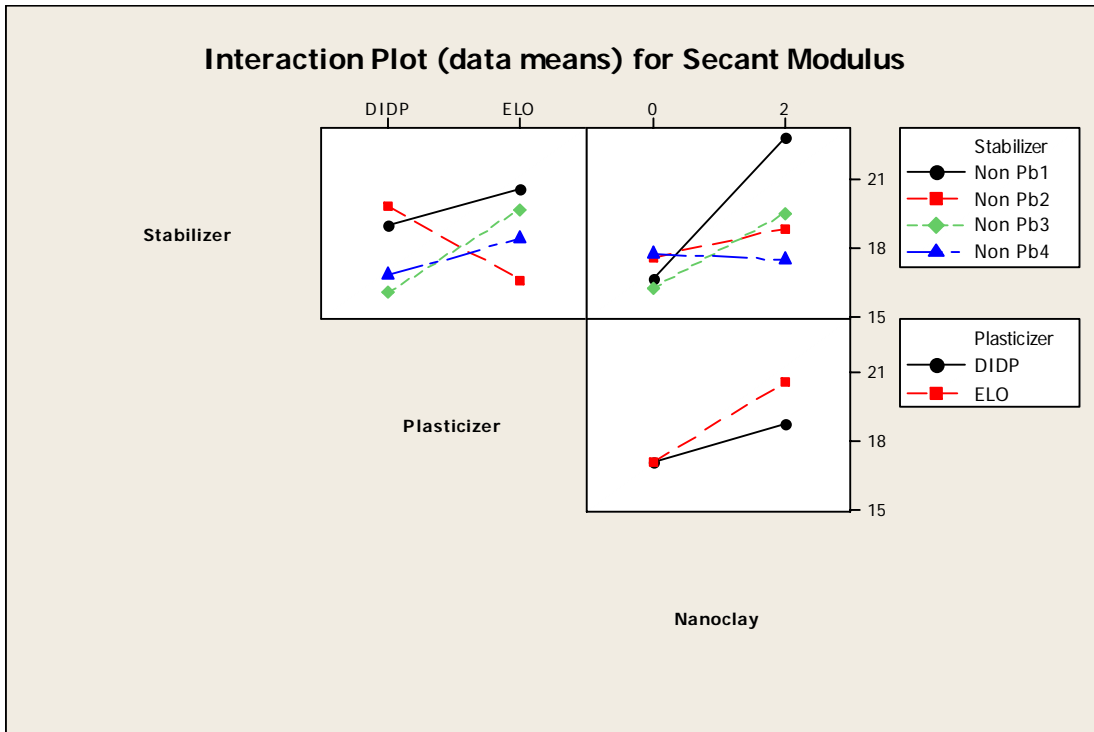


Figure G – 7 Shows the main effects plot for hardness

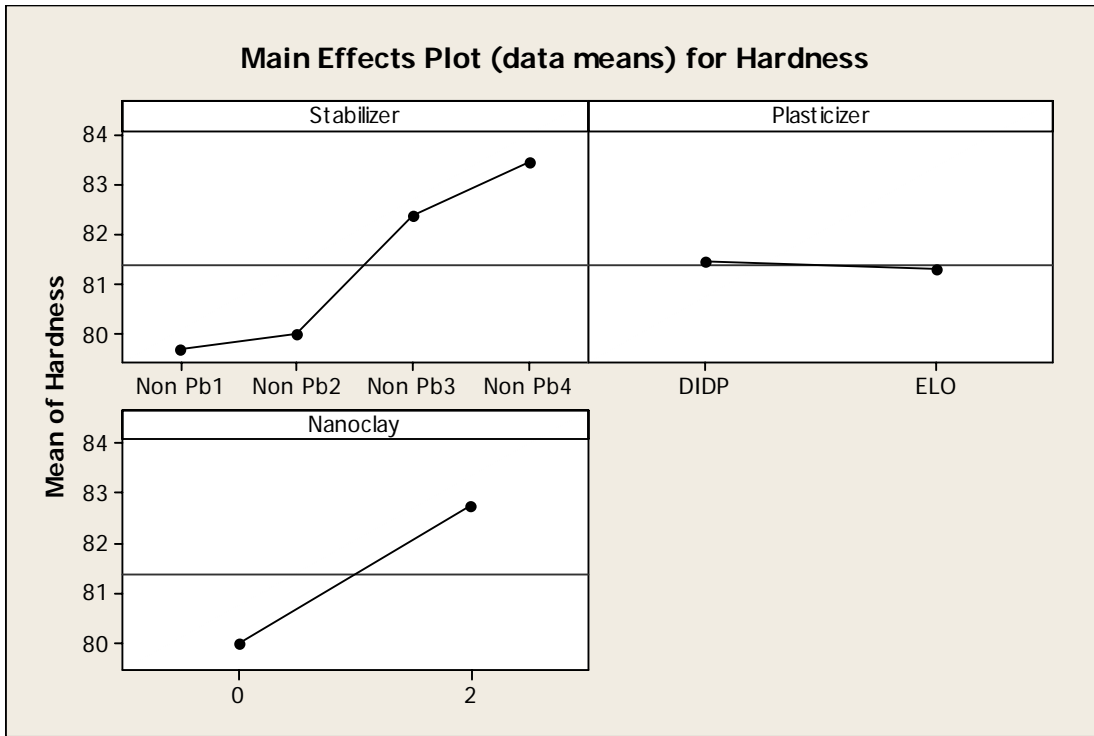


Figure G – 8 Shows the interaction effects plot for hardness

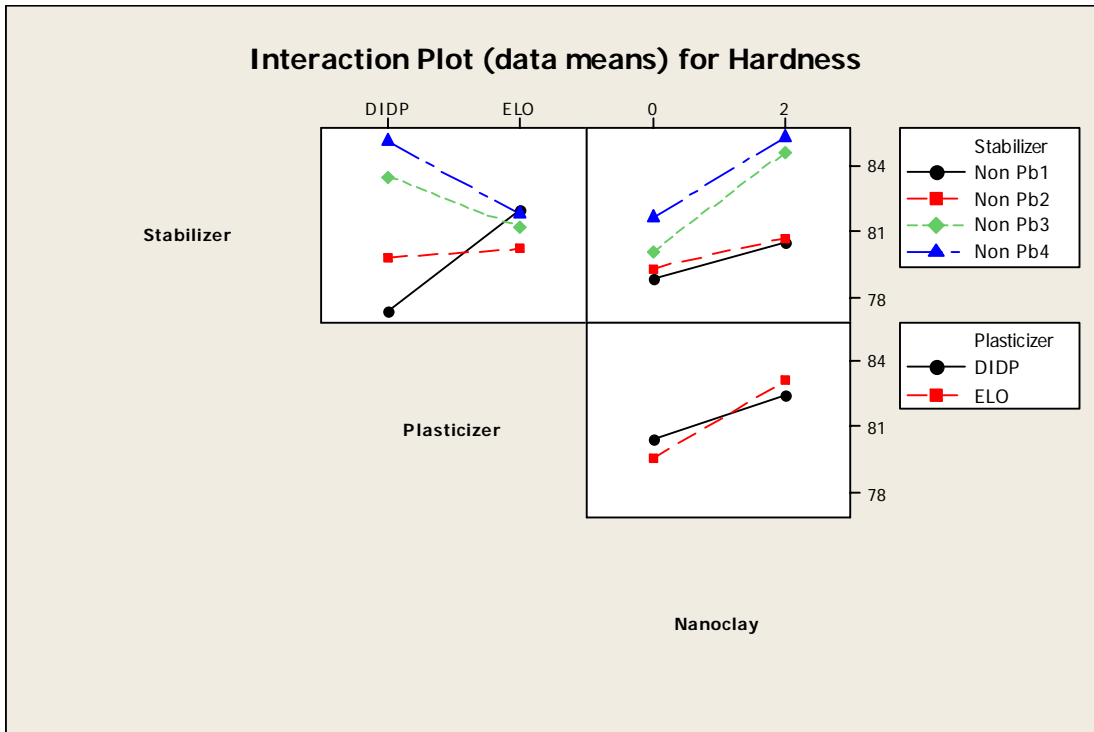


Figure H – 1 Shows the main effects plot for dynamic thermal stability

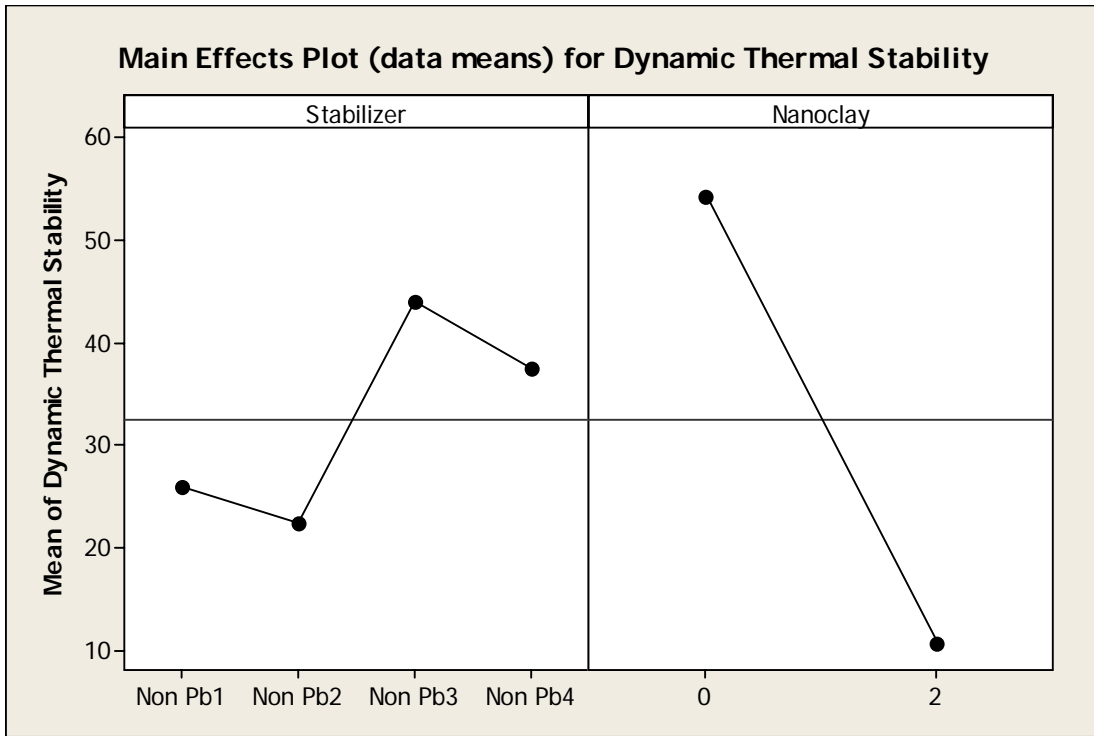


Figure H – 2 Shows the interaction effects plot for dynamic thermal stability

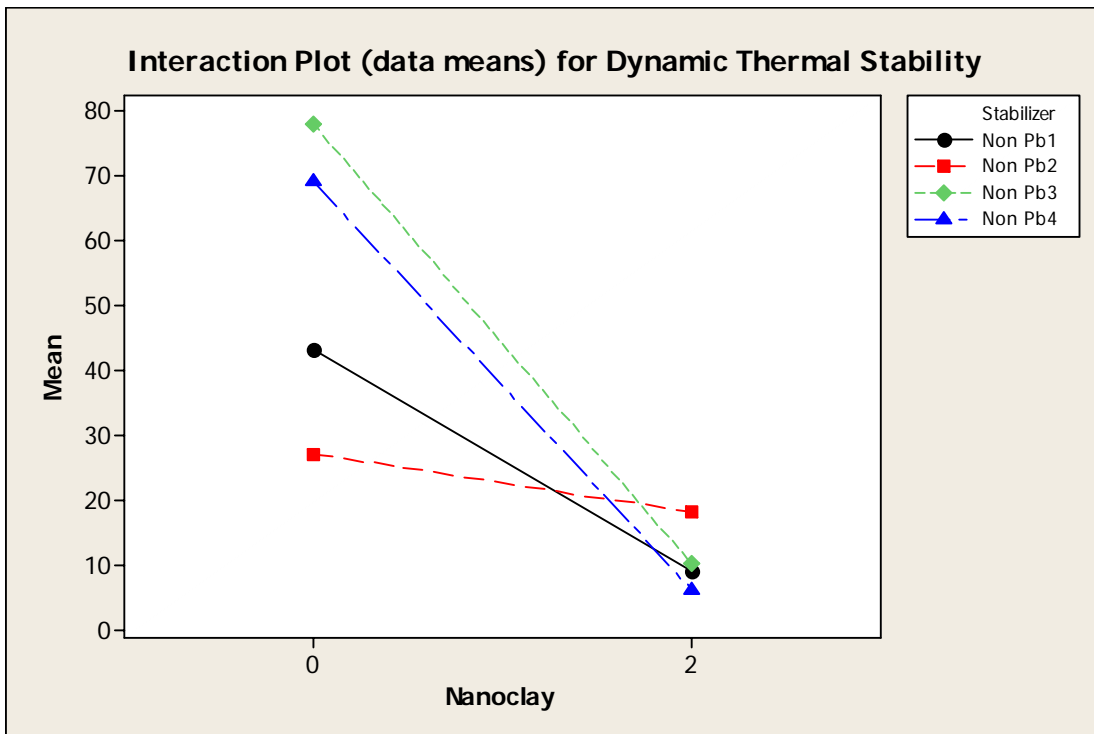


Figure I – 1 Shows the main effects plot for volume resistivity

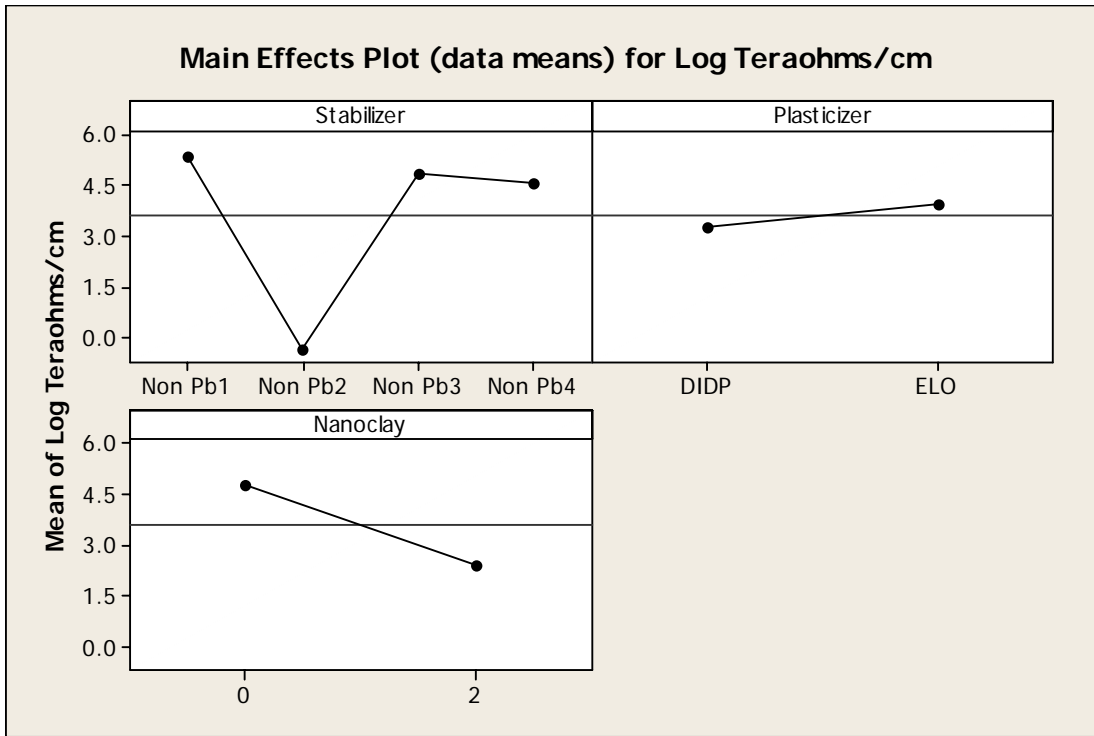


Figure I – 2 Shows the interaction effects plot for volume resistivity

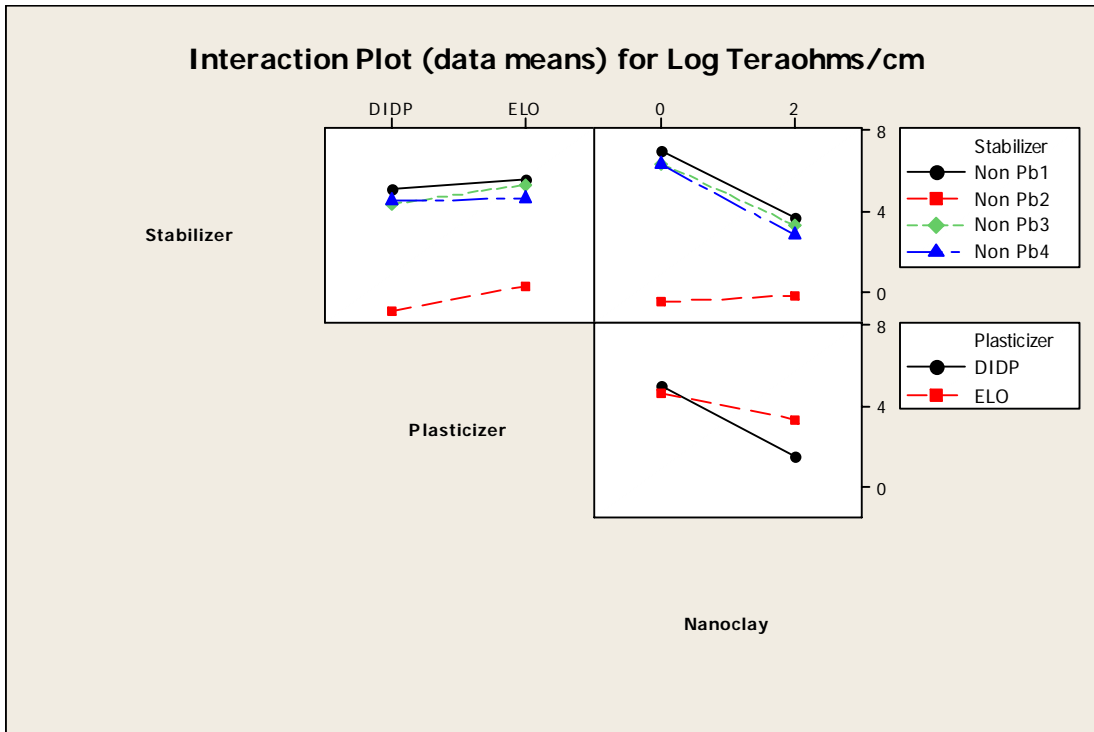


Figure J – 1 Shows the main effects plot for peak heat release rate

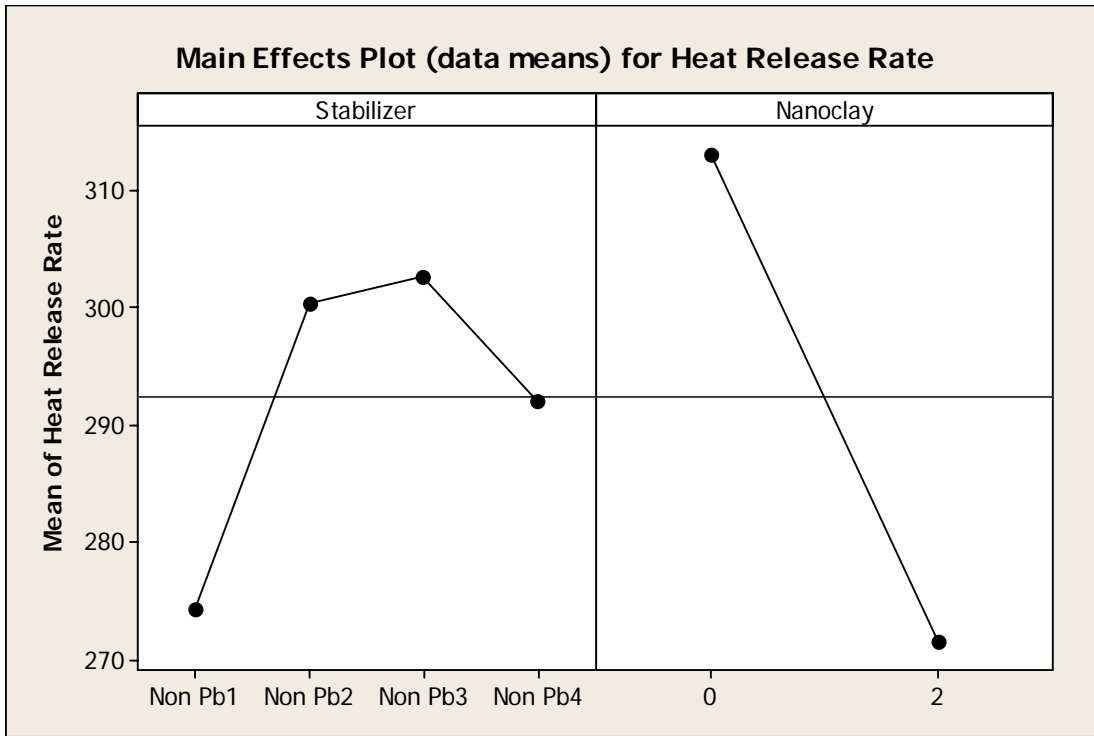


Figure J – 2 Shows the interaction effects plot for peak heat release rate

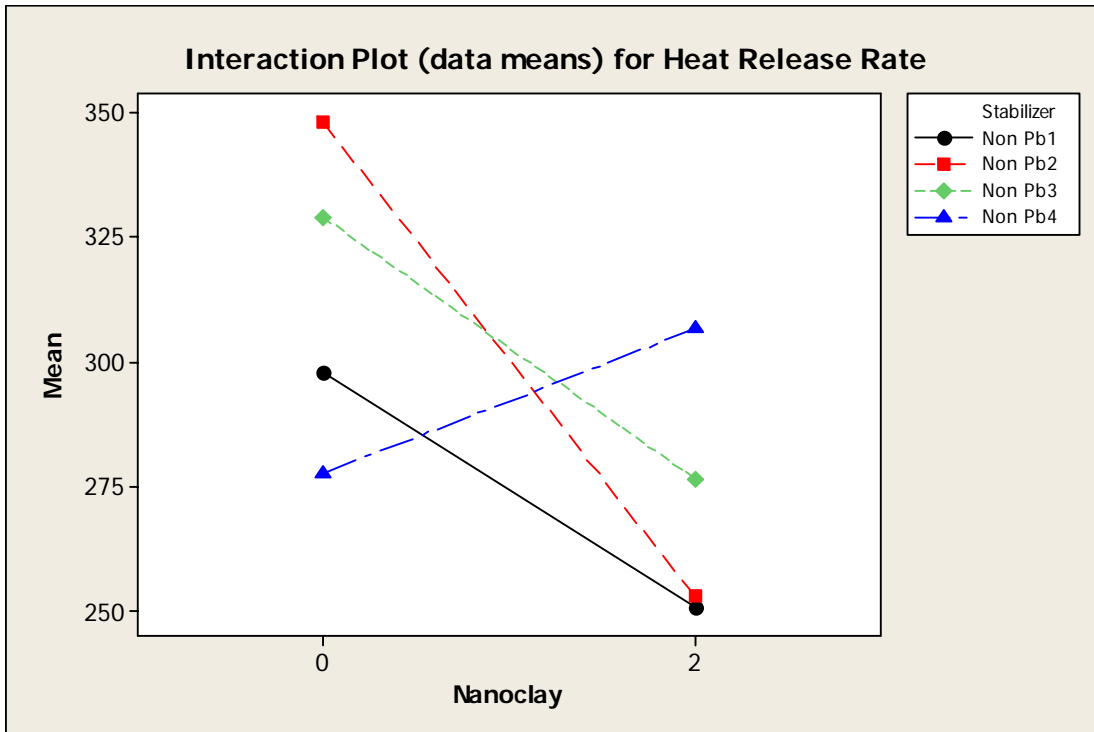


Figure J – 3 Shows the main effects plot for limiting oxygen index

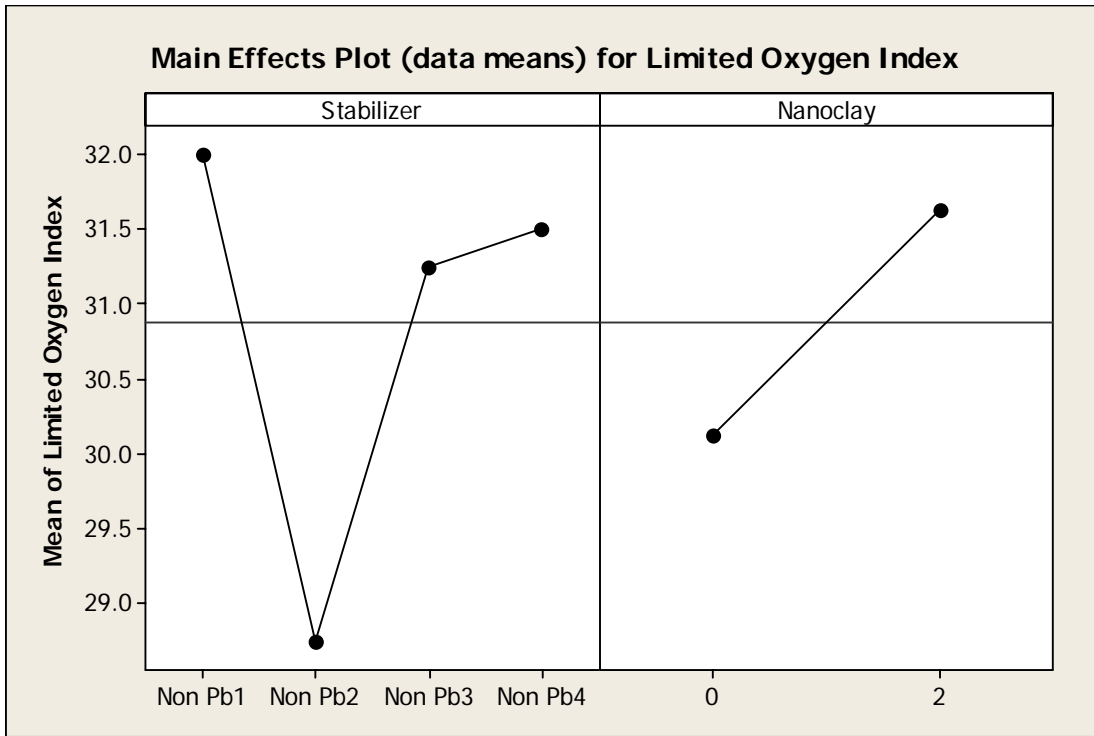


Figure J – 4 Shows the interaction effects plot for limiting oxygen index

